

Fig. 3. Inhibition of miR-122a by Ad vector-mediated TuD-122a expression. (A) Structure of the reporter gene-expressing plasmids psiCheck-2 and psiCheck-122aT. (B and C) Relative renilla luciferase expression levels following transduction with Ad-TuD-NC or Ad-TuD-122a at MOIs of 25 (B) and 100 (C). The data are expressed as the means \pm S.D. ($n=4$).

firefly luciferase expression levels were determined. Ad-TuD-122a significantly reduced the firefly luciferase expression levels in a dose-dependent manner (Fig. 4a). The firefly luciferase expression level was reduced to 29% of that in the cells transduced with Ad-TuD-NC at MOI of 100 by transduction with Ad-TuD-122a at MOI of 100. In contrast, no significant changes in the firefly luciferase expression were found by transduction with Ad-TuD-NC.

To examine whether inhibition of miR-122a by Ad vector-mediated TuD-122a expression leads to a reduction in HCV replicon RNA levels, strand-specific real-time RT-PCR analysis was performed to determine the HCV replicon RNA levels. Briefly, Huh-7.5.1 1bFeo cells were transduced with the Ad vectors as described above, and the total RNA was isolated 48 h after transduction. Real-time RT-PCR analysis for the HCV positive-strand RNA genome was performed as follows. Briefly, 2 μ g of total RNA was reverse-transcribed to cDNA using the primer specific for the HCV positive-strand genome (RC21; 5'-ctc ccg ggg cac tcg caa gc-3'). Real-time RT-PCR was performed using the primers (RC21 and RC1; 5'-gtc tag cca tgg cgt tag ta-3') and SYBR Premix Ex Taq II (Takara Bio Inc., Kyoto, Japan). Similarly to the results for the firefly luciferase expression in Fig. 4A, HCV replicon RNA levels were significantly reduced by Ad-TuD-122a (Fig. 4B). There was an approximately 2.2-fold decline in the HCV replicon RNA level in the cells transduced with Ad-TuD-122a at an MOI of 100, compared with the HCV replicon RNA level in the cells transduced with Ad-TuD-NC at an MOI of 100. Ad-TuD-NC did not apparently decrease the HCV replicon RNA levels. These results indicate that the inhibition of miR-122a by Ad vector-mediated TuD-122a expression efficiently suppresses the replication of the HCV replicon.

The present study demonstrates that Ad vector-mediated TuD-122a expression significantly inhibits the function of miR-122a and

replication of the HCV replicon. Replication of the HCV genome is promoted by the direct interaction between miR-122a and the complementary sequences in the 5'-UTR of the HCV genome (Henke et al., 2008; Jangra et al., 2010), indicating that sequestration of miR-122a leads to suppression of the HCV replication. In order to suppress the HCV replicon by inhibiting miR-122a, TuD-RNA was selected as an inhibitor of miRNA in this study, because TuD-RNA potentially inhibits miRNA by strongly binding to miRNA (Haraguchi et al., 2009). In addition, TuD-RNA can be expressed by conventional gene delivery vectors, including virus vectors. One drawback of TuD-RNA is that TuD-RNA does not discriminate miRNA members that belong to the same miRNA family (Haraguchi et al., 2009); however, miR-122a does not constitute a family of miRNA, suggesting that TuD-122a would not inhibit other miRNAs.

As described above, an Ad vector is suitable for liver-specific expression of TuD-RNA due to the strong hepatotropism. Previous studies demonstrated that Ad vectors expressing short-hairpin RNA (shRNA) or antisense RNA against the HCV genome successfully exhibited the suppressive effects on HCV infection in vivo (Gonzalez-Carmona et al., 2011; Sakamoto et al., 2008). Another advantage of using an Ad vector for treatment of HCV-related diseases is that in vivo administration of an Ad vector induces type I interferon (IFN) production via innate immune responses (Huarte et al., 2006; Zhu et al., 2007). Our group previously demonstrated that VA-RNA, which is a small non-coding RNA expressed from a replication-incompetent Ad vector as well as wild-type Ad, stimulates type I IFN production in an IFN- β promoter stimulator-1 (IPS-1)-dependent manner (Yamaguchi et al., 2010). Ad vector-induced type I IFN would contribute to suppression of HCV infection. The anti-HCV activity of Ad-TuD-122a can also be up-regulated by insertion of an expression cassette of an

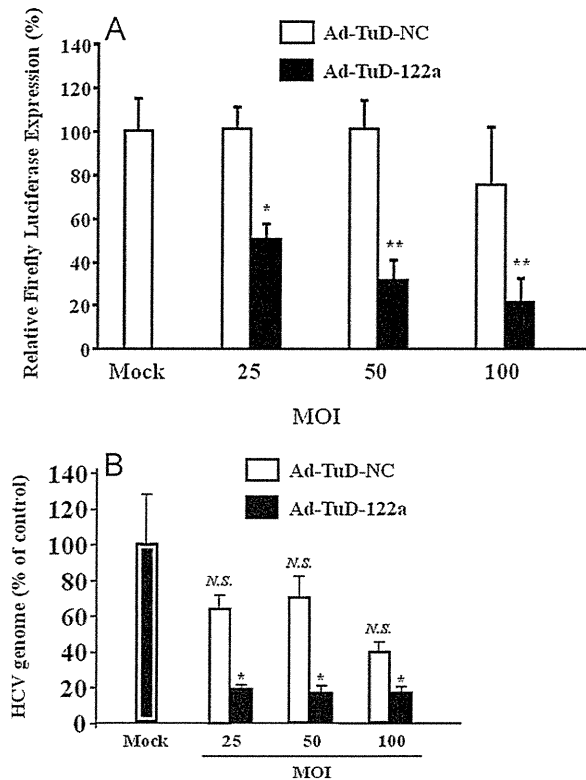


Fig. 4. Suppression of the HCV replicon by Ad vector-mediated TuD-122a expression. (A) Firefly luciferase expression levels and (B) HCV replicon RNA levels in Huh-7.5.1 1bFeo cells following transduction with the Ad vectors. All the data are shown as the means \pm S.D. ($n=3$). N.S.: not significant. * $P<0.05$, ** $P<0.005$ between mock-transduced cells and cells transduced with Ad-TuD-122a.

anti-HCV gene, including type I IFN genes and short-hairpin RNA (shRNA) or antisense RNA against the HCV genome, into the Ad vector genome. Our group has developed various types of Ad vectors in which two or three transgene expression cassettes can be inserted into a single Ad vector genome (Mizuguchi et al., 2001, 2005, 2003).

Previous studies have demonstrated that lipid droplets, which are lipid-storage intracellular organelles, are crucial for the production of infectious HCV particles (Hinson and Cresswell, 2009; Miyanari et al., 2007). Miyanari et al. demonstrated that HCV capsid proteins recruit the non-structural proteins and the replication complex to the lipid droplet-associated membrane (Miyanari et al., 2007). miR-122a is an important factor that regulates cholesterol and fatty-acid metabolism in the hepatocytes (Esau et al., 2006; Iliopoulos et al., 2010). Intravenous administration of the antisense oligonucleotide against miR-122a resulted in a reduction in the plasma levels of cholesterol and triglycerides (Esau et al., 2006; Lanford et al., 2010). In addition to the enhancement of accumulation and translation of the HCV genome, miR-122a might up-regulate HCV infection by regulating lipid metabolism in the hepatocytes.

Almost similar levels of reduction in the HCV replicon RNA copy numbers were found for Ad-TuD-122a at MOIs of 25, 50, and 100, although there was dose-dependent reduction in the firefly luciferase expression following transduction with Ad-TuD-122a. It remains unclear why dose-dependent reduction in the HCV replicon RNA copy numbers was not found, however, miR-122a plays a crucial role in the enhancement of both translation and stability of HCV genome (Henke et al., 2008; Jopling et al., 2005; Randall et al., 2007; Shimakami et al., 2012). Stability of HCV genome might be more susceptible to inhibition of miR-122a than translation. The averages of HCV replicon RNA levels were also reduced following transduction with Ad-TuD-NC, although

statistically significant differences were not found, compared with the mock-transduced cells. Replication-incompetent Ad vectors express non-coding small RNA (VA-RNA), which forms RNA-induced silencing complex (RISC) with argonaute 2 (Ago2) (Xu et al., 2007). Ago2 is an important factor for miRNA processing (Diederichs and Haber, 2007). Processing of miR-122a might be slightly disturbed by Ad vector-expressed VA-RNA, leading to the reduction in the HCV replicon RNA levels.

In summary, we efficiently suppressed the HCV replicon levels by Ad vector-mediated expression of TuD-122a, which blocks the function of miR-122a. This study indicates that Ad vector-mediated expression of TuD-122a in liver hepatocytes would offer an alternative approach for the treatment of HCV infection.

Conflict of interest

The authors declare no conflict of interest.

Acknowledgements

This study was supported by grants from the Ministry of Health, Labor and Welfare of Japan (to F.S.).

Appendix A. Supplementary data

Supplementary data associated with this article can be found, in the online version, at doi:10.1016/j.virusres.2012.02.003.

References

- Chisari, F.V., 2005. Unscrambling hepatitis C virus–host interactions. *Nature* 436 (7053), 930–932.
- Diederichs, S., Haber, D.A., 2007. Dual role for argonautes in microRNA processing and posttranscriptional regulation of microRNA expression. *Cell* 131 (6), 1097–1108.
- Esau, C., Davis, S., Murray, S.F., Yu, X.X., Pandey, S.K., Pear, M., Watts, L., Booten, S.L., Graham, M., McKay, R., Subramaniam, A., Propp, S., Lollo, B.A., Freier, S., Bennett, C.F., Bhanot, S., Monia, B.P., 2006. miR-122 regulation of lipid metabolism revealed by in vivo antisense targeting. *Cell Metab.* 3 (2), 87–98.
- Feld, J.J., Hoofnagle, J.H., 2005. Mechanism of action of interferon and ribavirin in treatment of hepatitis C. *Nature* 436 (7053), 967–972.
- Fluiter, K., ten Asbroek, A.L., de Wissel, M.B., Jakobs, M., Wissenbach, M., Olsson, H., Olsen, O., Oerum, H., Baas, F., 2003. In vivo tumor growth inhibition and biodistribution studies of locked nucleic acid (LNA) antisense oligonucleotides. *Nucleic Acids Res.* 31 (3), 953–962.
- Gonzalez-Carmona, M.A., Vogt, A., Heinicke, T., Quasdorff, M., Hoffmann, P., Yildiz, Y., Schneider, C., Serwe, M., Bartenschlager, R., Sauerbruch, T., Caselmann, W.H., 2011. Inhibition of hepatitis C virus gene expression by adenoviral vectors encoding antisense RNA in vitro and in vivo. *J. Hepatol.* 55 (1), 19–28.
- Haraguchi, T., Ozaki, Y., Iba, H., 2009. Vectors expressing efficient RNA decoys achieve the long-term suppression of specific microRNA activity in mammalian cells. *Nucleic Acids Res.* 37 (6), e43.
- Henke, J.L., Goergen, D., Zheng, J., Song, Y., Schuttler, C.G., Fehr, C., Junemann, C., Niepmann, M., 2008. microRNA-122 stimulates translation of hepatitis C virus RNA. *EMBO J.* 27 (24), 3300–3310.
- Hinson, E.R., Cresswell, P., 2009. The antiviral protein, viperin, localizes to lipid droplets via its N-terminal amphipathic alpha-helix. *Proc. Natl. Acad. Sci. U.S.A.* 106 (48), 20452–20457.
- Hoofnagle, J.H., 2002. Course and outcome of hepatitis C. *Hepatology* 36 (5 Suppl 1), S21–S29.
- Huarte, E., Larrea, E., Hernandez-Alcoceba, R., Alfaro, C., Murillo, O., Arina, A., Tirapu, I., Azpilicueta, A., Hervas-Stubbis, S., Bortolanza, S., Perez-Gracia, J.L., Civeira, M.P., Prieto, J., Riezu-Boj, J.I., Melerio, I., 2006. Recombinant adenoviral vectors turn on the type I interferon system without inhibition of transgene expression and viral replication. *Mol. Ther.* 14 (1), 129–138.
- Iliopoulos, D., Drosatos, K., Hiyama, Y., Goldberg, I.J., Zannis, V.I., 2010. MicroRNA-370 controls the expression of microRNA-122 and Cpt1alpha and affects lipid metabolism. *J. Lipid Res.* 51 (6), 1513–1523.
- Jangra, R.K., Yi, M., Lemon, S.M., 2010. Regulation of hepatitis C virus translation and infectious virus production by the microRNA miR-122. *J. Virol.* 84 (13), 6615–6625.
- Jopling, C.L., Yi, M., Lancaster, A.M., Lemon, S.M., Sarnow, P., 2005. Modulation of hepatitis C virus RNA abundance by a liver-specific MicroRNA. *Science* 309 (5740), 1577–1581.
- Krutzfeldt, J., Rajewsky, N., Braich, R., Rajeev, K.G., Tuschl, T., Manoharan, M., Stoffel, M., 2005. Silencing of microRNAs in vivo with 'antagomirs'. *Nature* 438 (7068), 685–689.

- Lanford, R.E., Hildebrandt-Eriksen, E.S., Petri, A., Persson, R., Lindow, M., Munk, M.E., Kauppinen, S., Orum, H., 2010. Therapeutic silencing of microRNA-122 in primates with chronic hepatitis C virus infection. *Science* 327 (5962), 198–201.
- Machlin, E.S., Sarnow, P., Sagan, S.M., 2011. Masking the 5' terminal nucleotides of the hepatitis C virus genome by an unconventional microRNA–target RNA complex. *Proc. Natl. Acad. Sci. U.S.A.* 108 (8), 3193–3198.
- Miyanari, Y., Atsuzawa, K., Usuda, N., Watashi, K., Hishiki, T., Zayas, M., Bartenschlager, R., Wakita, T., Hijikata, M., Shimotohno, K., 2007. The lipid droplet is an important organelle for hepatitis C virus production. *Nat. Cell Biol.* 9 (9), 1089–1097.
- Mizuguchi, H., Kay, M.A., Hayakawa, T., 2001. In vitro ligation-based cloning of foreign DNAs into the E3 and E1 deletion regions for generation of recombinant adenovirus vectors. *Biotechniques* 30 (5), 1112–1114, 1116.
- Mizuguchi, H., Xu, Z.L., Sakurai, F., Kawabata, K., Yamaguchi, T., Hayakawa, T., 2005. Efficient regulation of gene expression using self-contained fiber-modified adenovirus vectors containing the tet-off system. *J. Control. Release* 110 (1), 202–211.
- Mizuguchi, H., Xu, Z.L., Sakurai, F., Mayumi, T., Hayakawa, T., 2003. Tight positive regulation of transgene expression by a single adenovirus vector containing the rTA and tTS expression cassettes in separate genome regions. *Hum. Gene Ther.* 14 (13), 1265–1277.
- Randall, G., Panis, M., Cooper, J.D., Tellinghuisen, T.L., Sukhodolets, K.E., Pfeffer, S., Landthaler, M., Landgraf, P., Kan, S., Lindenbach, B.D., Chien, M., Weir, D.B., Russo, J.J., Ju, J., Brownstein, M.J., Sheridan, R., Sander, C., Zavolan, M., Tuschl, T., Rice, C.M., 2007. Cellular cofactors affecting hepatitis C virus infection and replication. *Proc. Natl. Acad. Sci. U.S.A.* 104 (31), 12884–12889.
- Roberts, A.P., Lewis, A.P., Jopling, C.L., 2011. miR-122 activates hepatitis C virus translation by a specialized mechanism requiring particular RNA components. *Nucleic Acids Res.*
- Sakamoto, N., Tanabe, Y., Yokota, T., Satoh, K., Sekine-Osajima, Y., Nakagawa, M., Itsui, Y., Tasaka, M., Sakurai, Y., Cheng-Hsin, C., Yano, M., Ohkoshi, S., Aoyagi, Y., Maekawa, S., Enomoto, N., Kohara, M., Watanabe, M., 2008. Inhibition of hepatitis C virus infection and expression in vitro and in vivo by recombinant adenovirus expressing short hairpin RNA. *J. Gastroenterol. Hepatol.* 23 (9), 1437–1447.
- Shimakami, T., Yamane, D., Jangra, R.K., Kempf, B.J., Spaniel, C., Barton, D.J., Lemon, S.M., 2012. Stabilization of hepatitis C virus RNA by an Ago2–miR-122 complex. *Proc. Natl. Acad. Sci. U.S.A.*
- Suzuki, T., Sakurai, F., Nakamura, S., Kouyama, E., Kawabata, K., Kondoh, M., Yagi, K., Mizuguchi, H., 2008. miR-122a-regulated expression of a suicide gene prevents hepatotoxicity without altering antitumor effects in suicide gene therapy. *Mol. Ther.* 16 (10), 1719–1726.
- Wilson, J.A., Zhang, C., Huys, A., Richardson, C.D., 2011. Human Ago2 is required for efficient microRNA 122 regulation of hepatitis C virus RNA accumulation and translation. *J. Virol.* 85 (5), 2342–2350.
- Xu, N., Segerman, B., Zhou, X., Akusjarvi, G., 2007. Adenovirus virus-associated RNAI-derived small RNAs are efficiently incorporated into the RNA-induced silencing complex and associate with polyribosomes. *J. Virol.* 81 (19), 10540–10549.
- Yamaguchi, T., Kawabata, K., Kouyama, E., Ishii, K.J., Katayama, K., Suzuki, T., Kurachi, S., Sakurai, F., Akira, S., Mizuguchi, H., 2010. Induction of type I interferon by adenovirus-encoded small RNAs. *Proc. Natl. Acad. Sci. U.S.A.* 107 (40), 17286–17291.
- Yokota, T., Sakamoto, N., Enomoto, N., Tanabe, Y., Miyagishi, M., Maekawa, S., Yi, L., Kurosaki, M., Taira, K., Watanabe, M., Mizusawa, H., 2003. Inhibition of intracellular hepatitis C virus replication by synthetic and vector-derived small interfering RNAs. *EMBO Rep.* 4 (6), 602–608.
- Zhu, J., Huang, X., Yang, Y., 2007. Innate immune response to adenoviral vectors is mediated by both Toll-like receptor-dependent and -independent pathways. *J. Virol.* 81 (7), 3170–3180.

Original Article

Factors responsible for the discrepancy between *IL28B* polymorphism prediction and the viral response to peginterferon plus ribavirin therapy in Japanese chronic hepatitis C patients

Hiroaki Saito,^{1,2} Kiyooki Ito,¹ Masaya Sugiyama,¹ Teppei Matsui,¹ Yoshihiko Aoki,¹ Masatoshi Imamura,¹ Kazumoto Murata,¹ Naohiko Masaki,¹ Hideyuki Nomura,³ Hiroshi Adachi,⁴ Shuhei Hige,⁵ Nobuyuki Enomoto,⁶ Naoya Sakamoto,⁷ Masayuki Kurosaki,⁸ Masashi Mizokami¹ and Sumio Watanabe²

¹The Research Center for Hepatitis and Immunology, National Center for Global Health and Medicine, Ichikawa, ²Department of Gastroenterology, Juntendo University School of Medicine, Bunkyo-ku, ³The Center for Liver Diseases, Shin-Kokura Hospital, Kitakyushu, Fukuoka, ⁴Department of Virology and Liver Unit, Tonami General Hospital, Tonami, ⁵Department of Internal Medicine, Hokkaido University Graduate School of Medicine, Sapporo, ⁶Department of Internal Medicine, University of Yamanashi, Kofu, ⁷Department for Hepatitis Control, Tokyo Medical and Dental University, Tokyo, and ⁸Division of Gastroenterology and Hepatology, Musashino Red Cross Hospital, Musashino, Japan

Aim: *IL28B* polymorphisms serve to predict response to pegylated interferon plus ribavirin therapy (PEG IFN/RBV) in Japanese patients with chronic hepatitis C (CHC) very reliably. However, the prediction by the *IL28B* polymorphism contradicted the virological response to PEG IFN/RBV in some patients. Here, we aimed to investigate the factors responsible for the discrepancy between the *IL28B* polymorphism prediction and virological responses.

Methods: CHC patients with genotype 1b and high viral load were enrolled in this study. In a case–control study, clinical and virological factors were analyzed for 130 patients with rs8099917 TT genotype and 96 patients with rs8099917 TG or GG genotype who were matched according to sex, age, hemoglobin level and platelet count.

Results: Higher low-density lipoprotein (LDL) cholesterol, lower γ -glutamyltransferase and the percentage of wild-type phenotype at amino acids 70 and 91 were significantly

associated with the rs8099917 TT genotype. Multivariate analysis showed that rs8099917 TG or GG genotype, older age and lower LDL cholesterol were independently associated with the non-virological responder (NVR) phenotype. In patients with rs8099917 TT genotype (predicted as virological responder [VR]), multivariate analysis showed that older age was independently associated with NVR. In patients with rs8099917 TG or GG genotype (predicted as NVR), multivariate analysis showed that younger age was independently associated with VR.

Conclusion: Patient age gave rise to the discrepancy between the prediction by *IL28B* polymorphism and the virological responses, suggesting that patients should be treated at a younger age.

Key words: aging, genotype, *IL28B*, low-density lipoprotein cholesterol, single nucleotide polymorphism

INTRODUCTION

HEPATITIS C VIRUS (HCV) infection is a global health problem with worldwide estimates of

120–130 million carriers.¹ Chronic HCV infection, the leading cause of liver transplantation, can lead to progressive liver disease, resulting in cirrhosis and complications, including decompensated liver disease and hepatocellular carcinoma.² The current standard-of-care treatment for suitable patients with chronic HCV infection consists of pegylated interferon- α -2a or -2b (PEG IFN) given by injection in combination with oral ribavirin (RBV) for 24 or 48 weeks, depending on HCV genotype. Large-scale treatment in the USA and Europe showed that 42–52% of patients with HCV genotype 1

Correspondence: Dr Masashi Mizokami, The Research Center for Hepatitis and Immunology, National Center for Global Health and Medicine, 1-7-1 Kohnodai, Ichikawa, Chiba 272-8516, Japan. Email: mmizokami@hospk.ncgm.go.jp

Received 23 February 2012; revision 18 March 2012; accepted 22 March 2012.

achieved a sustained virological response (SVR),^{3–5} and studies conducted in Japan produced similar results. This treatment is associated with well-known side-effects (e.g. influenza-like syndrome, hematological abnormalities and neuropsychiatric events) resulting in reduced compliance and fewer patients completing treatment.⁶ It is important to predict an individual's response before treatment with PEG IFN/RBV to avoid side-effects, as well as to reduce the treatment cost. The HCV genotype, in particular, is used to predict the response: patients with the HCV genotype 2/3 have a relatively high rate of SVR (70–80%) with 24 weeks of treatment, whereas those infected with genotype 1 have a much lower rate of SVR, despite 48 weeks of treatment.⁵

Our recent genome-wide association studies (GWAS) revealed that several highly correlated common single nucleotide polymorphisms (SNP) in the region of the interleukin-28B (*IL28B*) gene on chromosome 19, coding for interferon (IFN)- λ 3, are implicated in the non-virological responder (NVR) to PEG IFN/RBV phenotype among patients infected by HCV genotype 1.⁷ The association between response to PEG IFN/RBV and SNP associated with *IL28B* was concurrently reported by two other groups who also employed GWAS.^{8,9} The *IL28B* polymorphism was highly predictive of the response to PEG IFN/RBV therapy in Japanese chronic hepatitis C (CHC) patients.^{10–12} However, this was not always the case. Therefore, we attempted to determine why the *IL28B* polymorphism did not predict the response of all patients. The nature of the functional link between the *IL28B* polymorphism and HCV clearance is unknown, and this must be defined to understand how the *IL28B* polymorphism correlates with HCV clearance. Therefore, we also investigated the association between the *IL28B* polymorphism and clinical characteristics of CHC patients.

METHODS

Patients

A TOTAL OF 696 CHC patients with genotype 1b and high viral load were recruited from the National Center for Global Health and Medicine, Hokkaido University Hospital, Tokyo Medical and Dental University Hospital, Yamanashi University Hospital, Tonami General Hospital, and Shin-Kokura Hospital in Japan. In a case-control study, sex, age, hemoglobin level and platelet count were matched between patients with the rs8099917 TT genotype ($n = 130$) and patients with

rs8099917 TG or GG genotypes ($n = 96$) to eliminate background biases.

Each patient was treated with PEG IFN- α -2b (1.5 μ g/kg s.c. weekly) or PEG IFN- α -2a (180 μ g/body s.c. weekly) plus RBV (600–1000 mg daily, depending on bodyweight). Because a reduction in the dose of PEG IFN/RBV can contribute to a lower SVR rate,¹³ only patients with an adherence of more than 80% dose for both drugs during the first 12 weeks were included in this study. Those positive for hepatitis B surface antigen and/or anti-HIV were excluded from this study.

Non-virological response was defined as less than a 2 log-unit decline in the serum level of HCV RNA from the pretreatment baseline value within the first 12 weeks and detectable viremia 24 weeks after treatment. Virological response (VR) was defined as attaining SVR or transient virological response (TVR) in this study; SVR was defined as undetectable HCV RNA in serum 6 months after treatment, whereas TVR was defined as a reappearance of HCV RNA in serum after the treatment was discontinued for a patient who had undetectable HCV RNA during the therapy or on completion of the therapy. At the time of enrollment, written informed consent was obtained for the collection and storage of serum and peripheral blood. This study was conducted in accordance with provisions of the Declaration of Helsinki.

Clinical and laboratory data

The sex, age, hemoglobin (Hb) and platelet counts were matched between study groups. Other parameters determined were as follows: alkaline phosphatase (ALP), alanine transaminase (ALT), total cholesterol, fasting blood sugar (FBS), low-density lipoprotein (LDL) cholesterol, γ -glutamyl transpeptidase (γ -GTP), α -fetoprotein (AFP), HCV RNA level and the rs8099917 polymorphism near *IL28B*.

DNA extraction

Genomic DNA was extracted from the buffy coat fraction of patients' whole blood using a GENOMIX kit (Talent SRL; Trieste, Italy).

IL28B genotyping

We have reported that the rs8099917 polymorphism is the best predictor for the response of Japanese CHC patients to PEG IFN/RBV therapy than other SNP near *IL28B*.¹⁴ Therefore, the rs8099917 polymorphism was genotyped using the InvaderPlus assay (Third Wave Japan, Tokyo, Japan), which combines polymerase

chain reaction (PCR) and the invader reaction.^{15,16} The InvaderPlus assay was performed using the LightCycler LC480 (Roche Applied Science, Mannheim, Germany).

Detection of amino acid substitutions in core and NS5A regions of HCV-1b

In the present study, substitutions of amino acid residues 70 (s-aa 70) and 91 (s-aa 91), and the presence of the IFN sensitivity-determining region (ISDR) were determined by direct nucleotide sequencing. HCV RNA was extracted from serum samples at the start of patients' therapy and reverse transcribed with a random primer and SuperScript III reverse transcriptase (Life Technologies, Carlsbad, CA, USA). Nucleic acids were amplified by PCR as described.¹⁷

Statistical analysis

Quantitative variables were expressed as the mean \pm standard error (SE) unless otherwise specified. Categorical variables were compared using a χ^2 -test or Fisher's exact test, as appropriate, and continuous variables were compared using the Mann–Whitney *U*-test. $P < 0.05$ was considered statistically significant. Multivariate analysis was performed using a stepwise logistic regression model. We performed statistical analyses using STATA ver. 11.0 (StataCorp, College Station, TX, USA).

RESULTS

Patient characteristics and *IL28B* genotype in a matched case–control study

TABLE 1 SHOWS PATIENT characteristics according to *IL28B* genotype. In a matched case–control study, sex, age, Hb levels and platelet counts were matched between 130 patients with rs8099917 TT genotype and 96 patients with rs8099917 TG or GG genotype. Lower γ -GTP ($P = 0.013$) and higher LDL cholesterol levels ($P < 0.001$) were significantly associated with the TT genotype of rs8099917. The percentages of wild type of s-aa 70 and s-aa 91 of patients with the rs8099917 TT genotype were significantly higher than those of patients with rs8099917 TG or GG genotype (s-aa 70: TT vs TG + GG, 68% vs 37% [$P < 0.001$]; s-aa 91: TT vs TG + GG, 68% vs 51% [$P = 0.017$]).

Factors associated with NVR in total patients

Table 2 shows the factors associated with NVR by univariate and multivariate analyses. Univariate analysis showed that older age ($P = 0.002$), lower platelet counts ($P = 0.01$), higher γ -GTP ($P = 0.013$), lower total cholesterol ($P = 0.017$), lower LDL cholesterol ($P < 0.001$) levels and higher AFP levels ($P = 0.019$) were significantly associated with NVR. The percentage of TG or GG genotype of rs8099917 of patients with NVR was

Table 1 Univariate analysis of *IL28B* TT and TG + GG genotypes

Variable	TT genotype (<i>n</i> = 130)	TG + GG genotype (<i>n</i> = 96)	<i>P</i> -value
Sex (% male)	61 (47)	46 (48)	Matched
Age (years), mean (SE)	57.2 (0.8)	57.5 (0.9)	Matched
Hemoglobin (g/dL), mean (SE)	14.3 (0.3)	13.9 (0.2)	Matched
Platelet count (μ L), mean (SE)	16.2 (0.5)	16.0 (0.5)	Matched
ALT (IU/L), mean (SE)	79.4 (5.4)	80.5 (7.8)	0.281
ALP (IU/L), mean (SE)	273.8 (11.7)	283.9 (11.8)	0.313
γ -GTP (IU/L), mean (SE)	63.4 (6.0)	76.0 (6.4)	0.013
Total cholesterol (mg/dL), mean (SE)	177.5 (3.3)	172.3 (3.2)	0.345
LDL cholesterol (mg/dL), mean (SE)	99.0 (2.6)	83.5 (2.8)	<0.001
Fasting blood sugar (mg/dL), mean (SE)	114.1 (4.1)	104.4 (1.9)	0.97
AFP (ng/dL), mean (SE)	9.8 (1.1)	11.5 (1.6)	0.190
HCV RNA (log IU), mean (SE)	6.2 (0.1)	6.1 (0.1)	0.186
s-aa 70 wild type (%)	70/103 (68)	30/81 (37)	<0.001
s-aa 91 wild type (%)	70/103 (68)	41/81 (51)	0.017
ISDR mutation 0–1 point (%)	82/100 (82)	70/81 (86)	0.42

AFP, α -fetoprotein; ALP, alkaline phosphatase; ALT, alanine aminotransferase; γ -GTP, γ -glutamyl transpeptidase; HCV, hepatitis C virus; ISDR, interferon sensitivity-determining region; LDL, low-density lipoprotein; SE, standard error.

Table 2 Univariate and multivariate analyses of patients with chronic hepatitis C treated with PEG IFN/RBV with respect to VR and NVR

Variable	Univariate analysis			Multivariate analysis	
	VR (n = 128)	NVR (n = 98)	P-value	OR (95% CI)	P-value
Sex (% male)	65 (51)	42 (43)	0.237		
Age (years), mean (SE)	55.6 (0.8)	59.6 (0.9)	0.002	1.075 (1.012–1.143)	0.02
rs8099917 (TG or GG genotype) (%)	23/128 (18)	73/98 (74)	<0.001	25.460 (7.436–87.169)	<0.001
Hemoglobin (g/dL), mean (SE)	14.4 (0.3)	13.7 (0.2)	0.053		
Platelet count (/μL), mean (SE)	16.9 (0.5)	15.0 (0.5)	0.01		
ALT (IU/L), mean (SE)	83.9 (6.4)	74.5 (6.2)	0.116		
ALP (IU/L), mean (SE)	274.1 (12.3)	282.9 (11.2)	0.169		
γ-GTP (IU/L), mean (SE)	65.9 (6.4)	72.6 (5.6)	0.013		
Total cholesterol (mg/dL), mean (SE)	180.3 (3.1)	168.4 (3.5)	0.017		
LDL cholesterol (mg/dL), mean (SE)	100.5 (2.7)	83.5 (2.8)	<0.001	0.978 (0.956–0.999)	0.046
Fasting blood sugar (mg/dL), mean (SE)	106.6 (2.9)	114.8 (4.4)	0.058		
AFP (ng/dL), mean (SE)	9.6 (1.1)	12.0 (1.6)	0.021		
HCV RNA (Log IU), mean (SE)	6.2 (0.1)	6.2 (0.1)	0.876		
s-aa 70 wild type (%)	67/102 (66)	33/82 (54)	0.001		
s-aa 91 wild type (%)	67/102 (66)	44/82 (54)	0.097		
ISDR mutation 0–1 point (%)	79/96 (82)	73/85 (86)	0.511		

AFP, α-fetoprotein; ALP, alkaline phosphatase; ALT, alanine aminotransferase; CI, confidence interval; γ-GTP, γ-glutamyl transpeptidase; HCV, hepatitis C virus; ISDR, interferon sensitivity-determining region; LDL, low-density lipoprotein; NVR, non-virological response; OR, odds ratio; PEG IFN, peginterferon; SE, standard error; RBV, ribavirin; VR, virological response.

significantly higher than that of patients with VR (VR vs NVR: 23/128 [18%] vs 73/98 [74%], $P < 0.001$). The percentage of wild-type s-aa 70 in patients with NVR was significantly lower than that in patients with VR [VR vs NVR: 67/102 [66%] vs 33/82 [54%], $P = 0.001$]. Multivariate analysis showed that older age (odds ratio [OR] = 1.075; 95% confidence interval [CI] = 1.012–1.14; $P = 0.02$), TG or GG genotype of rs8099917 (OR = 25.460; 95% CI = 7.436–87.169; $P < 0.001$) and lower LDL cholesterol levels (OR = 0.978; 95% CI = 0.956–0.999; $P = 0.046$) were independently associated with NVR.

VR to treatment depending on *IL28B* genotype

In the patients with the rs8099917 TT genotype, the rates of SVR, TVR and NVR were 62%, 19% and 19%, respectively. Therefore, 19% patients were NVR, even though rs8099917 represents the TT genotype (predicted as VR). In contrast, in the patients with rs8099917 TG or GG, the rates of SVR, TVR and NVR were 14%, 10% and 76%, respectively. Therefore, 24% patients were VR, even though rs8099917 was TG or GG genotype (predicted as NVR) (Fig. 1).

Factors associated with NVR in patients with the rs8099917 TT genotype

Table 3 shows the factors associated with NVR in patients with the rs8099917 TT genotype (predicted as VR) by univariate and multivariate analyses. Univariate analysis showed that female sex ($P = 0.003$), older age

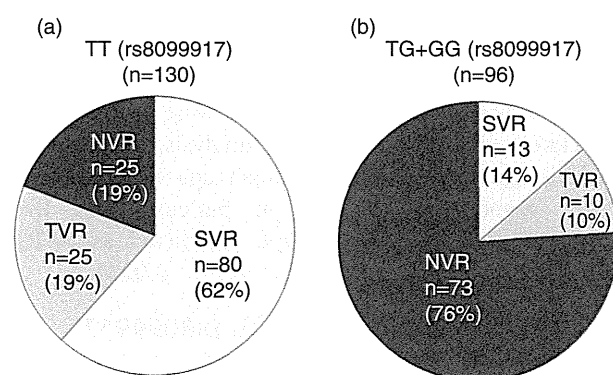


Figure 1 Virological responses to pegylated interferon and ribavirin therapy were shown in patients with rs8099917 TT (a) and TG + GG (b). NVR, non-virological response; SVR, sustained virological response; TVR, transient virological response.

Table 3 Variables associated with NVR by univariate and multivariate analyses in patients with rs8099917 TT genotype

Variable	Univariate analysis			Multivariate analysis	
	VR (<i>n</i> = 105)	NVR (<i>n</i> = 25)	<i>P</i> -value	OR (95% CI)	<i>P</i> -value
Sex (% male)	56 (53)	5 (20)	0.003		
Age (years), mean (SE)	56.1 (0.8)	61.7 (1.6)	0.001	1.142 (1.026–1.271)	0.015
Hemoglobin (g/dL), mean (SE)	14.6 (0.4)	13.1 (0.3)	0.005		
Platelet count (/μL), mean (SE)	16.7 (0.6)	13.8 (1.0)	0.019		
ALT (IU/L), mean (SE)	83.6 (6.3)	61.0 (7.9)	0.053		
ALP (IU/L), mean (SE)	270.6 (13.6)	285.9 (22.3)	0.206		
γ-GTP (IU/L), mean (SE)	66.9 (7.1)	49.2 (7.4)	0.473		
Total cholesterol (mg/dL), mean (SE)	180.2 (3.6)	165.0 (7.6)	0.072		
LDL cholesterol (mg/dL), mean (SE)	101.2 (2.9)	88.5 (5.2)	0.067		
Fasting blood sugar (mg/dL), mean (SE)	108.4 (3.5)	140.0 (15.5)	0.127		
AFP (ng/dL), mean (SE)	9.4 (1.2)	12.2 (3.6)	0.245		
HCV RNA (log IU), mean (SE)	6.2 (0.1)	6.2 (0.1)	0.948		
s-aa 70 wild type (%)	57/83 (66)	13/20 (75)	0.752		
s-aa 91 wild type (%)	55/83 (66)	15/20 (75)	0.452		
ISDR mutation 0–1 point (%)	64/79 (81)	18/21 (86)	0.618		

AFP, α -fetoprotein; ALP, alkaline phosphatase; ALT, alanine aminotransferase; CI, confidence interval; γ -GTP, γ -glutamyl transpeptidase; HCV, hepatitis C virus; ISDR, interferon sensitivity-determining region; LDL, low-density lipoprotein; NVR, non-virological response; OR, odds ratio; SE, standard error; VR, virological response.

($P = 0.001$), lower Hb levels ($P = 0.005$) and lower platelet counts ($P = 0.019$) were significantly associated with NVR in patients with the rs8099917 TT genotype. Multivariate analysis showed that only older age was independently associated with NVR in patients with the rs8099917 TT genotype (predicted as VR) (OR = 1.142; 95% CI = 1.026–1.27; $P = 0.015$).

Factors associated with VR in patients with the rs8099917 TG or GG genotypes

Table 4 shows the factors associated with VR in patients with the rs8099917 TG or GG genotypes (predicted as NVR) by univariate and multivariate analyses. Younger age ($P = 0.005$), lower γ -GTP ($P = 0.009$) and higher LDL cholesterol levels ($P = 0.032$) were significantly associated with VR by univariate analysis. Multivariate analysis showed that only younger age was independently associated with VR in patients with the rs8099917 TG or GG genotype (predicted as NVR) (OR = 0.926; 95% CI = 0.867–0.990; $P = 0.023$).

Rate of VR depending on the rs8099917 genotype of each age group

We divided patients into four age groups and compared VR rates by the differences in rs8099917 genotype for each group. The rate of VR decreased gradually in the older age groups independent of genotype. In the less than 49 years age group, the rate of VR in patients with

the rs8099917 TT genotype was significantly higher than that in patients with the rs8099917 TG + GG genotypes ($P = 0.0002$). Further, in the 50–59 and 60–69 years age groups, the rates of VR in patients with the rs8099917 TT genotype were significantly higher than those in patients with the rs8099917 TG + GG genotypes ($P < 0.0001$, respectively). In the group that included subjects aged older than 69 years, only 50% of patients achieved VR even in those with the rs8099917 TT genotype (predicted as VR). In contrast, 47.6% of patients achieved VR, including those with the rs8099917 TG or GG genotypes (predicted as NVR) in the less than 49 years group (Fig. 2).

DISCUSSION

SINGLE NUCLEOTIDE POLYMORPHISM array analysis employing GWAS technology conducted by our laboratory and others revealed the relationships between SNP associated with the *IL28B* locus or present within the coding sequences for IFN- λ 3, or the response to PEG IFN/RBV therapy for CHC.^{7–9} Subsequent studies have confirmed that the response to PEG IFN/RBV therapy correlates with the SNP associated with *IL28B*^{18,19} and indicates their value for predicting the response to PEG IFN/RBV therapy. Unfortunately, these predictions do not hold for some patients. In an attempt to understand the reasons for this, in the present study,

Table 4 Variables associated with VR by univariate and multivariate analyses in patients with rs8099917 TG or GG genotypes

Variable	Univariate analysis			Multivariate analysis	
	VR (n = 23)	NVR (n = 73)	P-value	OR (95% CI)	P-value
Sex (% male)	9 (40%)	37 (51%)	0.333		
Age (years), mean (SE)	53.2 (1.7)	58.8 (1.1)	0.005	0.926 (0.867–0.990)	0.023
Hemoglobin (g/dL), mean (SE)	13.6 (0.3)	13.9 (0.2)	0.44		
Platelet count (/μL), mean (SE)	17.6 (1.1)	15.5 (0.6)	0.059		
ALT (IU/L), mean (SE)	85.5 (21.6)	78.9 (7.8)	0.767		
ALP (IU/L), mean (SE)	291.9 (28.6)	281.8 (13.0)	0.921		
γ-GTP (IU/L), mean (SE)	62.2 (15.1)	80.4 (6.9)	0.009		
Total cholesterol (mg/dL), mean (SE)	180.5 (6.2)	169.5 (3.7)	0.17		
LDL cholesterol (mg/dL), mean (SE)	97.6 (6.9)	81.9 (3.6)	0.032		
Fasting blood sugar (mg/dL), mean (SE)	98.1 (2.8)	106.3 (2.3)	0.084		
AFP (ng/dL), mean (SE)	10.3 (3.4)	11.9 (1.8)	0.123		
HCV RNA (log IU), mean (SE)	5.9 (0.1)	6.2 (0.1)	0.087		
s-aa 70 wild type (%)	10/19 (53)	20/62 (32)	0.108		
s-aa 91 wild type (%)	12/19 (63)	29/62 (47)	0.211		
ISDR mutation 0–1 point (%)	15/17 (88)	55/64 (86)	0.806		

AFP, α-fetoprotein; ALP, alkaline phosphatase; ALT, alanine aminotransferase; CI, confidence interval; γ-GTP, γ-glutamyl transpeptidase; HCV, hepatitis C virus; ISDR, interferon sensitivity-determining region; LDL, low-density lipoprotein; NVR, non-virological response; OR, odds ratio; SE, standard error; VR, virological response.

we recruited a new set of patients for further analysis. Here, we confirmed that *IL28B* polymorphism was the most significant predictive factor for NVR with respect to PEG IFN/RBV treatment. Moreover, 19% of patients exhibiting the rs8099917 TT genotype were NVR,

although they were predicted as VR. Twenty-four percent of patients with the rs8099917 TG or GG genotypes were VR, although they were predicted as NVR. We were able to determine by multivariate analysis that age was the most likely factor responsible for the discordance

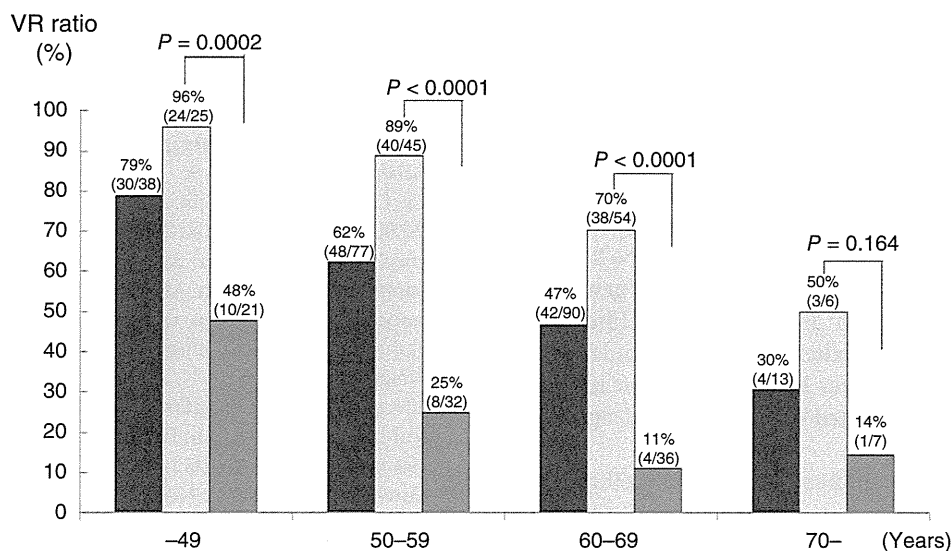


Figure 2 Virological responses (VR) to pegylated interferon and ribavirin therapy were compared between the patients with rs8099917 TT and TG + GG in each generation group. (■) Total patients, (□) TT genotype (rs8099917), (▒) TG + GG genotype (rs8099917).

between *IL28B* genotype and patients' response to viral infection.

How does age influence the VR to PEG IFN/RBV therapy? First, the lower rate of VR to PEG IFN/RBV therapy in patients with CHC was attributed to lower compliance with the IFN or RBV dose.^{20,21} Because lower compliance with PEG IFN or RBV therapy was expected to be associated with a lower rate of VR in older patients, we recruited patients who were administered over 80% of the prescribed dose of IFN/RBV. Therefore, lower compliance can be discounted as a reason for reduced response. Second, a more advanced stage of fibrosis might have been present in the older group. Platelet counts in patients with NVR were significantly lower than those in patients with VR, and lower platelet counts may be associated with advanced fibrosis.²² Moreover, advanced fibrosis is associated with lower rates of SVR to IFN-based therapy.²³ Third, epigenetic factors such as DNA methylation induced by aging may be involved in the reduced efficacy of PEG IFN/RBV treatment in older patients. DNA methylation near gene promoters is known to turn off transcription or reduce it considerably,²⁴ and advanced age is strongly associated with the increased DNA methylation.²⁵ Therefore, DNA methylation may be increased near or in the *IL28B* promoter as a function of age resulting in suppression of *IL28B* transcription.

Lower LDL cholesterol levels were significantly associated with NVR in patients with CHC. Moreover, LDL cholesterol levels in patients with the rs8099917 TT genotype were significantly higher than those in patients with the TG + GG genotypes. The association between LDL cholesterol and *IL28B* polymorphism as well as the VR to PEG IFN/RBV has been reported.²⁶ Higher pre-treatment levels of LDL cholesterol have been shown to predict increased response to standard PEG IFN/RBV treatment for patients with CHC.^{27,28} Although the mechanisms responsible for the association between LDL cholesterol levels and the VR to PEG IFN/RBV are unknown, the *IL28B*-rs8099917 TT responder genotype, which may correlate with an increased likelihood of treatment response and higher LDL cholesterol levels, is associated with either lower IFN- λ 3 activity or reduced expression of genes regulated by IFN-mediated signaling pathways.

In conclusion, our studies provide compelling evidence that patient age is most likely responsible for incorrect predictions of VR to PEG IFN/RBV therapy in Japanese CHC patients based on *IL28B* genotypes. Our findings indicated that patients should be treated as soon as they are diagnosed. It will be important to

investigate the role of the epigenetic factors associated with *IL28B* expression to develop more effective PEG IFN/RBV-based therapies for patients with CHC.

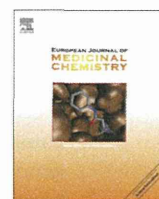
ACKNOWLEDGMENT

THIS STUDY WAS supported by grants (21-112 and 21-113) from the National Center for Global Health and Medicine in Japan.

REFERENCES

- 1 Global Burden of Hepatitis C Working Group. Global burden of disease (GBD) for hepatitis C. *J Clin Pharmacol* 2004; 44: 20–9.
- 2 Younossi Z, Kallman J, Kincaid J. The effects of HCV infection and management on health-related quality of life. *Hepatology* 2007; 45: 806–16.
- 3 Fried MW, Shiffman ML, Reddy KR *et al.* Peginterferon alfa-2a plus ribavirin for chronic hepatitis C virus infection. *N Engl J Med* 2002; 347: 975–82.
- 4 Manns MP, McHutchison JG, Gordon SC *et al.* Peginterferon alfa-2b plus ribavirin compared with interferon alfa-2b plus ribavirin for initial treatment of chronic hepatitis C: a randomised trial. *Lancet* 2001; 358: 958–65.
- 5 Hadziyannis SJ, Sette H, Jr, Morgan TR *et al.* Peginterferon-alpha2a and ribavirin combination therapy in chronic hepatitis C: a randomized study of treatment duration and ribavirin dose. *Ann Intern Med* 2004; 140: 346–55.
- 6 Bruno S, Camma C, Di Marco V *et al.* Peginterferon alfa-2b plus ribavirin for naive patients with genotype 1 chronic hepatitis C: a randomized controlled trial. *J Hepatol* 2004; 41: 474–81.
- 7 Tanaka Y, Nishida N, Sugiyama M *et al.* Genome-wide association of *IL28B* with response to pegylated interferon-alpha and ribavirin therapy for chronic hepatitis C. *Nat Genet* 2009; 41: 1105–9.
- 8 Ge D, Fellay J, Thompson AJ *et al.* Genetic variation in *IL28B* predicts hepatitis C treatment-induced viral clearance. *Nature* 2009; 461: 399–401.
- 9 Suppiah V, Moldovan M, Ahlenstiel G *et al.* *IL28B* is associated with response to chronic hepatitis C interferon-alpha and ribavirin therapy. *Nat Genet* 2009; 41: 1100–4.
- 10 Watanabe S, Enomoto N, Koike K *et al.* Cancer preventive effect of pegylated interferon alpha-2b plus ribavirin in a real-life clinical setting in Japan: PERFECT interim analysis. *Hepatol Res* 2011; 41: 955–64.
- 11 Kurosaki M, Tanaka Y, Nishida N *et al.* Pre-treatment prediction of response to pegylated-interferon plus ribavirin for chronic hepatitis C using genetic polymorphism in *IL28B* and viral factors. *J Hepatol* 2011; 54: 439–48.
- 12 Kurosaki M, Sakamoto N, Iwasaki M *et al.* Pretreatment prediction of response to peginterferon plus ribavirin

- therapy in genotype 1 chronic hepatitis C using data mining analysis. *J Gastroenterol* 2011; 46: 401–9.
- 13 McHutchison JG, Manns M, Patel K *et al.* Adherence to combination therapy enhances sustained response in genotype-1-infected patients with chronic hepatitis C. *Gastroenterology* 2002; 123: 1061–9.
 - 14 Ito K, Higami K, Masaki N *et al.* The rs8099917 polymorphism, when determined by a suitable genotyping method, is a better predictor for response to pegylated alpha interferon/ribavirin therapy in Japanese patients than other single nucleotide polymorphisms associated with interleukin-28B. *J Clin Microbiol* 2011; 49: 1853–60.
 - 15 Lyamichev V, Mast AL, Hall JG *et al.* Polymorphism identification and quantitative detection of genomic DNA by invasive cleavage of oligonucleotide probes. *Nat Biotechnol* 1999; 17: 292–6.
 - 16 Lyamichev VI, Kaiser MW, Lyamicheva NE *et al.* Experimental and theoretical analysis of the invasive signal amplification reaction. *Biochemistry* 2000; 39: 9523–32.
 - 17 Akuta N, Suzuki F, Hirakawa M *et al.* Amino acid substitution in hepatitis C virus core region and genetic variation near the interleukin 28B gene predict viral response to telaprevir with peginterferon and ribavirin. *Hepatology* 2010; 52: 421–9.
 - 18 Rauch A, Kutalik Z, Descombes P *et al.* Genetic variation in IL28B is associated with chronic hepatitis C and treatment failure: a genome-wide association study. *Gastroenterology* 2010; 138: 1338–45. 45 e1–7.
 - 19 Montes-Cano MA, Garcia-Lozano JR, Abad-Molina C *et al.* Interleukin-28B genetic variants and hepatitis virus infection by different viral genotypes. *Hepatology* 2010; 52: 33–7.
 - 20 Yamada G, Iino S, Okuno T *et al.* Virological response in patients with hepatitis C virus genotype 1b and a high viral load: impact of peginterferon-alpha-2a plus ribavirin dose reductions and host-related factors. *Clin Drug Investig* 2008; 28: 9–16.
 - 21 Bourliere M, Ouzan D, Rosenheim M *et al.* Pegylated interferon-alpha2a plus ribavirin for chronic hepatitis C in a real-life setting: the Hepatys French cohort (2003–2007). *Antivir Ther* 2012; 17: 101–10.
 - 22 Karasu Z, Tekin F, Ersoz G *et al.* Liver fibrosis is associated with decreased peripheral platelet count in patients with chronic hepatitis B and C. *Dig Dis Sci* 2007; 52: 1535–9.
 - 23 Everson GT, Hoefs JC, Seeff LB *et al.* Impact of disease severity on outcome of antiviral therapy for chronic hepatitis C: lessons from the HALT-C trial. *Hepatology* 2006; 44: 1675–84.
 - 24 Suzuki MM, Bird A. DNA methylation landscapes: provocative insights from epigenomics. *Nat Rev Genet* 2008; 9: 465–76.
 - 25 Boks MP, Derks EM, Weisenberger DJ *et al.* The relationship of DNA methylation with age, gender and genotype in twins and healthy controls. *PLoS ONE* 2009; 4: e6767.
 - 26 Li JH, Lao XQ, Tillmann HL *et al.* Interferon-lambda genotype and low serum low-density lipoprotein cholesterol levels in patients with chronic hepatitis C infection. *Hepatology* 2010; 51: 1904–11.
 - 27 Gopal K, Johnson TC, Gopal S *et al.* Correlation between beta-lipoprotein levels and outcome of hepatitis C treatment. *Hepatology* 2006; 44: 335–40.
 - 28 Toyoda H, Kumada T. Cholesterol and lipoprotein levels as predictors of response to interferon for hepatitis C. *Ann Intern Med* 2000; 133: 921.



Original article

Inhibition of hepatitis C virus NS5B polymerase by S-trityl-L-cysteine derivatives

Daniel B. Nichols^a, Guy Fournet^b, K.R. Gurukumar^a, Amartya Basu^a, Jin-Ching Lee^c, Naoya Sakamoto^d, Frank Kozielski^e, Ira Musmuca^f, Benoît Joseph^{b,**,}, Rino Ragno^{f,***}, Neerja Kaushik-Basu^{a,*}^a Department of Biochemistry and Molecular Biology, UMDNJ-New Jersey Medical School, 185 South Orange Avenue, Newark, NJ 07103, USA^b Institut de Chimie et Biochimie Moléculaires et Supramoléculaires, UMR-CNRS 5246, Université de Lyon, Université Claude Bernard – Lyon 1, Bâtiment Curien, 43 Boulevard du 11 Novembre 1918, F-69622 Villeurbanne, France^c Department of Biotechnology, College of Life Science, Kaohsiung Medical University, Kaohsiung, Taiwan^d Department of Gastroenterology and Hepatology, Tokyo Medical and Dental University, Tokyo 113-8519, Japan^e The Beatson Institute for Cancer Research, Molecular Motors Laboratory, Garscube Estate, Switchback Road, Bearsden, Glasgow G61 1BD, UK^f Rome Center for Molecular Design, Dipartimento di Chimica e Tecnologia del Farmaco, Sapienza Università di Roma, P.le A. Moro 5, 00185 Rome, Italy

ARTICLE INFO

Article history:

Received 20 December 2011

Received in revised form

3 January 2012

Accepted 5 January 2012

Available online 12 January 2012

Keywords:

Antiviral agents

Hepatitis C

HCV NS5B polymerase

Inhibitors

STLC derivatives

ABSTRACT

Structure-based studies led to the identification of a constrained derivative of S-trityl-L-cysteine (STLC) scaffold as a candidate inhibitor of hepatitis C virus (HCV) NS5B polymerase. A panel of STLC derivatives were synthesized and investigated for their activity against HCV NS5B. Three STLC derivatives, **9**, F-3070, and F-3065, were identified as modest HCV NS5B inhibitors with IC₅₀ values between 22.3 and 39.7 μM. F-3070 and F-3065 displayed potent inhibition of intracellular NS5B activity in the BHK-NS5B-FRLuc reporter and also inhibited HCV RNA replication in the Huh7/Rep-Feo1b reporter system. Binding mode investigations suggested that the STLC scaffold can be used to develop new NS5B inhibitors by further chemical modification at one of the trityl phenyl group.

© 2012 Elsevier Masson SAS. All rights reserved.

1. Introduction

Hepatitis C virus (HCV) infection represents a major public-health concern. It is estimated that over 200 million people, ~3% of the world population, are chronically infected with the virus [1–3]. HCV has an array of immune evasion strategies and can persist in the host for years. Individuals with chronic HCV infection are at increased risk of developing cirrhosis and hepatocellular carcinoma [3–7]. Currently, HCV infections are treated by a combination of pegylated-interferon, the nucleoside analog ribavirin, and one of two recently approved HCV protease inhibitors, Boceprevir or Telaprevir [8–13]. However, this therapy is limited in efficacy against the various HCV genotypes. Furthermore, in addition to its high cost, the current treatment is associated with severe side effects and a complicated dosing regimen that may limit patient compliance [11,12]. Also the possibility of selecting drug resistant HCV variants remains [12,13]. Therefore, the development

of additional, efficacious and more cost effective HCV antiviral therapies that target viral proteins and have limited effects on host biological processes is a priority.

HCV is a member of the *Flaviviridae* family. The positive sense, 9.6 kb RNA genome is translated into a single 3000 amino acid polyprotein via an IRES sequence located within the 5' non-translated region (NTR) of the viral genome [14,15]. The viral polyprotein is processed by both host and viral proteases into individual viral proteins consisting of four structural (core, E1, E2, and p7) and six nonstructural proteins (NS2, NS3, NS4A, NS4B, NS5A, and NS5B) [16]. HCV replicates exclusively in the cytoplasm of host cells. Replication of the viral RNA genome is mediated by the RNA-dependent RNA polymerase (RdRp) activity of the HCV nonstructural protein NS5B [17–19]. Because of the absolute requirement of NS5B to synthesize nascent HCV RNA, NS5B represents an attractive target for the development of anti-HCV inhibitors [20,21]. Furthermore, host cells lack RdRp. Therefore, an inhibitor that blocks RdRp activity should, in theory, have minimal or no effect on host biological processes. Though, a number of NIs and NNIs with potent *in vitro* anti-NS5B activity have been identified in recent years, they have presented challenges of toxicity and selection of resistant viruses, thus necessitating identification of better NS5B inhibitor scaffolds.

* Corresponding author. Tel.: +1 973 972 8653; fax: +1 973 972 5594.

** Corresponding author. Tel.: +33 4 72448135; fax: +33 4 72431214.

*** Corresponding author. Tel.: +396 4991 3937; fax: +396 4991 3627.

E-mail addresses: benoit.joseph@univ-lyon1.fr (B. Joseph), rino.ragno@uniroma1.it (R. Ragno), kaushik@umdnj.edu (N. Kaushik-Basu).

The structure of NS5B has been extensively characterized. The 66 kDa viral polymerase resembles a “right hand” with the active site contained in the palm domain and the RNA interacting region in the finger and thumb domains [22–25]. Current NS5B inhibitors can be divided into two classes, nucleoside inhibitors (NI) and non-nucleoside inhibitors (NNI). Once converted by host proteins into nucleotides, NIs cause RNA-chain termination upon incorporation by NS5B into the nascent RNA chains. NNIs bind to one of the five allosteric sites on NS5B and inhibit the initiation step of RNA synthesis.

Recently, we reported on the utility of three-dimensional quantitative structure-activity relationship (3D-QSAR) in combination with ligand-based and structure-based alignment procedures for *in silico* screening of new HCV NS5B polymerase inhibitors [26]. This investigation identified four new NS5B inhibitors from forty candidates examined from the NCI diversity set [26]. The most interesting hit, NSC123526 (Fig. 1), has been reported to be active against other viruses [27] and can be simply viewed as a constrained derivative of the *S*-trityl-L-cysteine (STLC) scaffold. STLC derivatives are versatile compounds endowed with antileukemic activity [28] and are also reported to inhibit the human mitotic kinesin Eg5 (HMKEg) by a non-competitive mechanism [29].

Herein, we describe molecular modeling studies that led us to explore the potential of STLC and its derivatives to inhibit HCV NS5B RdRp activity *in vitro*. Further, we examined the effect of STLC derivatives on intracellular HCV NS5B RdRp activity and on HCV RNA replication. Among the tested STLC derivatives, we identified three compounds as novel HCV NS5B inhibitor leads. These compounds merit further optimization through classical medicinal chemistry and virtual screening.

2. Results and discussion

2.1. Molecular modeling

Recently, we utilized structure-based 3-D QSAR modeling to identify NS5B thumb-binding inhibitors and reported on the identification of NSC123526 as a modest HCV NS5B inhibitor [26]. NSC123526 can be considered as a constrained STLC derivative (Fig. 1). Since STLC derivative NSC123139 (Fig. 1) was found to be most potent in inhibiting HMKEg, we performed cross-docking experiments to investigate whether it could also bind the HCV-NS5B thumb domain [26,29]. Fig. 2 depicts the docked conformation of NSC123139 in HCV-NS5B and HMKEg.

The activity of the docked NSC123139 (Predicted $pIC_{50} = 5.64$) was predicted by our 3-D QSAR model in the same range of NSC123526 (Experimental $pIC_{50} = 4.33$, predicted $pIC_{50} = 5.4$) [26]. However, NSC123139 exhibited a much weaker inhibition of NS5B RdRp activity *in vitro* (Table 1), compared to NSC123526, as previously reported [26].

Based on the above partial results, we tested a series of STLC derivatives for their ability to inhibit NS5B, with the objective of identifying new lead scaffolds. While our investigations with additional STLC derivatives were still ongoing, the co-crystal structures of HMKEg with NSC123139 (pdb entry code 2wog and 2xae) and other STLCs (2xr2 and 3ken) were released [30]. Nevertheless, docking calculations performed through Autodock Vina, were in good agreement with the experimental results ($rmsd = 0.44$) and with similar docking calculations previously reported [31], thus supporting our protocol.

The above docking protocol was also applied to the other STLCs. In addition, we analyzed the Autodock Vina proposed binding

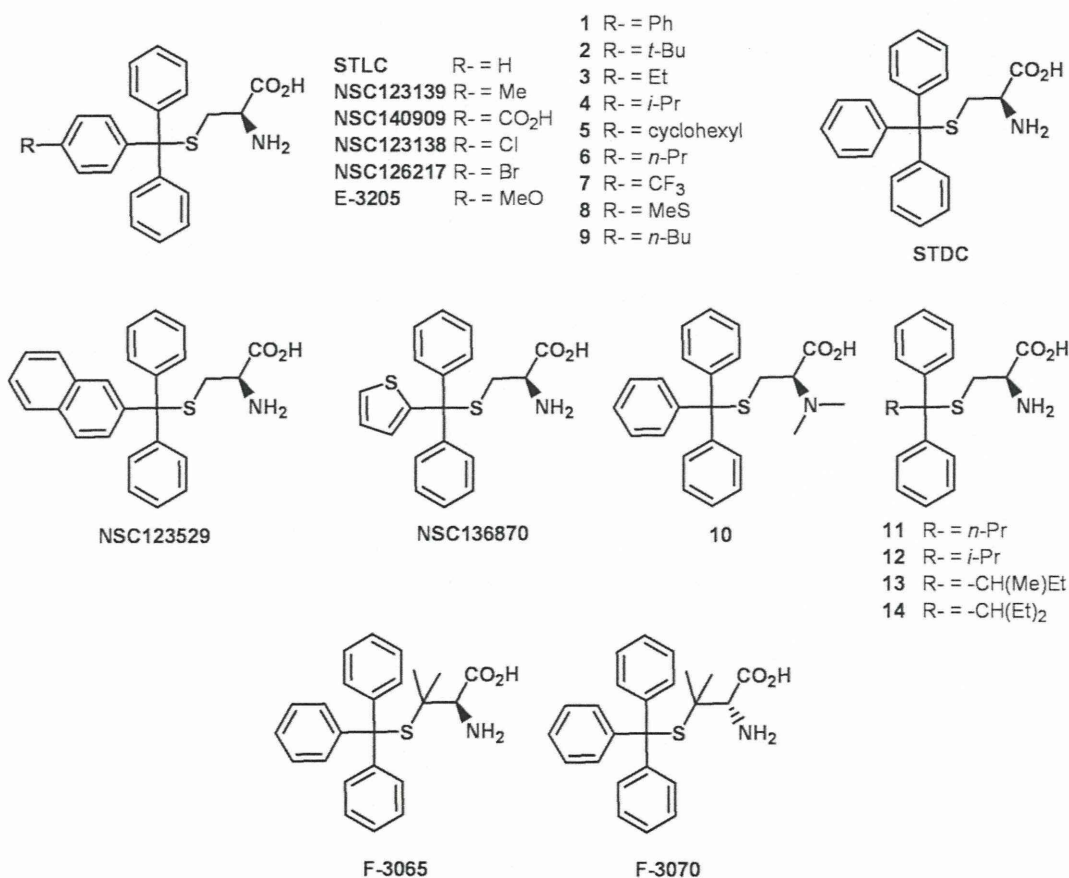


Fig. 1. Structures of NSC123526, STLC, STDC and STLC derivatives.

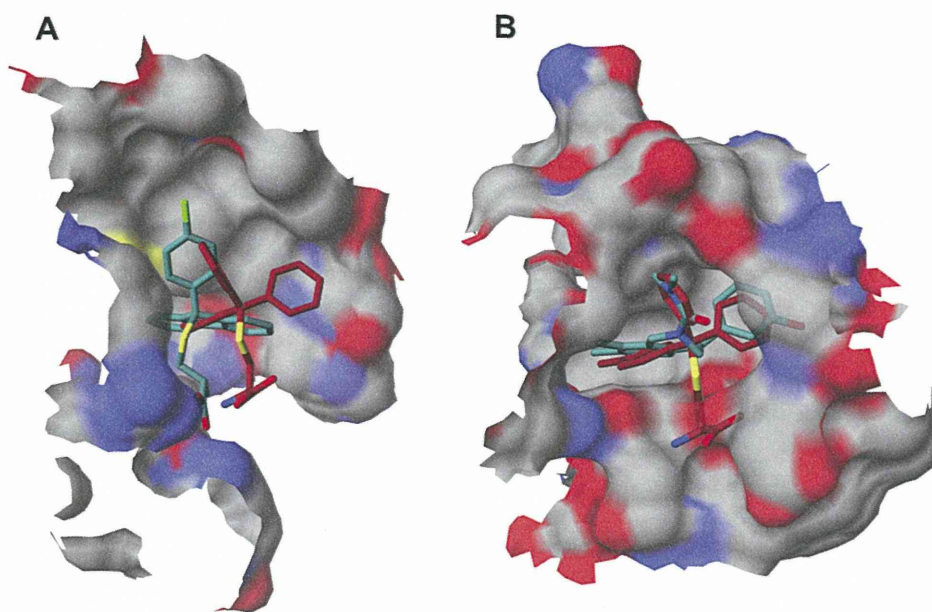


Fig. 2. Molecular docking of STL derivatives in NS5B. Panel A: Docked conformations of NSC123139 (red-colored carbon atoms) and NSC123526 (green-colored carbon atoms) within NS5B thumb domain. Panel B: HMKEg (PDB entry code 2fme) with docked conformation of NSC123139 (red-colored carbon atoms) and the experimental bound NSC123526 (green-colored carbon atoms). (For interpretation of the references to colour in this figure legend, the reader is referred to the web version of this article.)

mode of the two most active compounds, F-3065 and F-3070, cross-docked into the 15 NS5B-NNI co-crystal structures as previously described by us [26]. As expected, docked conformations of F-3065 and F-3070 ((*R*) and (*S*) enantiomers of the same compound, respectively) exhibited the lowest binding energy in the PDB entry 2d3u. Further, the bound conformations of F-3065 and F-3070, in agreement with the biological data, revealed that the cysteine stereocenter does not affect the overall binding mode, wherein the terminal amino acid group is involved in a hydrogen bonding network, as shown in the ligplot diagrams in Fig. 3. In particular the α -amino acid portion of F-3065 makes two hydrogen bonds, one between its amino group and the carbonyl group of Trp528 ($N\cdots O$ distance = 3.01 Å) and the other between a carboxy oxygen and the ϵ -amino group of Lys533 ($O\cdots N$ distance = 2.98 Å) (Fig. 3A). The ligplot diagram of the (*S*) enantiomer F-3070, that forms two hydrogen bonds with its two carboxy oxygens, one with the guanidinic nitrogen of Arg501 ($O\cdots N$ distance = 3.21 Å) and the other with ϵ -amino group of Lys533 ($O\cdots N$ distance 3.05–3.22 Å), is shown in Fig. 3B. This type of hydrogen bonding network was observed in all other STL derivatives (Fig. 5) suggesting that hydrogen bonds are the leading interactions.

Other notable interactions are hydrophobic in nature, and the trityl moieties are buried in the thumb allosteric binding side (Fig. 4). For both F-3065 and F-3070, one phenyl is placed in a pocket formed by Leu419, Arg422, Met423 and Trp528, while the other two benzenes fill-up two depressions on the enzyme surface. By comparing the binding mode of the most active STLs with that of the experimental co-crystallized compound found in 2d3u and considering the conserved binding modes shown in Fig. 5, we believe the STL can be used as a starting scaffold, whose activity could be improved by inserting a side chain in one of the two surface bound benzene rings to better fill the binding cleft formed by Leu419, Met423, Ile482, Val485, Ala486, Leu489 and Leu497 (Fig. 6) and occupied by a 2-(4-cyanophenyl)thiophene group in the original complex (PDB ID 2d3u). As expected and within the limit of any predictive model, the application of our 3-D QSAR to all the new STLs, predicted these compounds to have activities between the 10–100 μM range (data not shown).

2.2. Chemistry

A total of 35 STL derivatives were utilized in this study (Fig. 1 and Scheme 1). STL and 14 derivatives (**1–14**) have been reported previously [29,31]. Compounds F-3070 and F-3065 were purchased from Bachem, while STDC (NSC123676), NSC123139, NSC136870, NSC140909, NSC123529, NSC123138, and NSC126217 were procured from NCI/NIH. In accordance with published literature, 12 STL derivatives were newly synthesized for this investigation (Scheme 1). Starting aryldiphenylmethanol compounds **15** were prepared in good yields from appropriate esters (ArCO_2Me) and phenylmagnesium chloride (data not shown) [32]. Condensation of cysteamine.HCl (**16**) with $\text{Ar}(\text{Ph})_2\text{COH}$ ($\text{Ar} = 4\text{-Me-Ph}$, 4-Et-Ph , $4\text{-}n\text{-Pr-Ph}$, 4-MeS-Ph , 4-I-Ph , 4-(Ph)-Ph and 2-naphthyl) **15a–g** in TFA gave final compounds **17a–g** in 29–47% yield (Scheme 1). Treatment of *L*-cysteine (**18**) or *L*-penicillamine (**19**) with $\text{Ar}(\text{Ph})_2\text{COH}$ ($\text{Ar} = 4\text{-(}n\text{-C}_5\text{H}_{11}\text{)-Ph}$, $4\text{-(}n\text{-C}_6\text{H}_{13}\text{)-Ph}$, 4-PrO-Ph and $4\text{-}n\text{-Bu-Ph}$) **15h–k** in the presence of $\text{BF}_3\cdot\text{Et}_2\text{O}$ afforded target compounds **17h–l** in 30–55% yield (Scheme 1).

2.3. Biological studies

With the objective of identifying novel HCV NS5B inhibitors, we investigated STL and its derivatives employing the *in vitro* NS5B RdRp inhibition assay as described previously [33–35]. Recombinant HCV NS5B (genotype 1b) carrying an N-terminal His-tag and C-terminal 21-amino acid truncation (NS5BC Δ 21) was purified to homogeneity by Ni-NTA chromatography and used as a source of enzyme [33–35]. Wedelolactone, a documented NS5B inhibitor, was employed as an internal reference standard, and yielded an IC_{50} value of 36.0 μM (data not shown), consistent with our previously reported value [34]. In order to identify a wider range of NS5B inhibitor candidates, preliminary screening of STL and its derivatives was conducted at 100 μM compound concentration. While the parent STL molecule yielded only ~12% inhibition of NS5B RdRp activity during preliminary screening, its thirty-five derivatives, with the exception of **17l**, exhibited a much higher inhibition ranging from 14 to 83% (Table 1). Of these, three compounds **9**, F-

Table 1
Anti-HCV NS5B RdRp activity of STLC derivatives.

Compound	% Inhibition ^a	IC ₅₀ (μM) ^b
STLC	12.6 ± 2.3	n.d.
STDC	17.0 ± 0.6	n.d.
NSC123139	23.1 ± 1.6	n.d.
NSC136870	23.4 ± 2.9	n.d.
NSC140909	30.9 ± 3.7	n.d.
NSC123529	14.7 ± 1.5	n.d.
NSC123138	28.3 ± 5.9	n.d.
NSC126217	20.2 ± 2.5	n.d.
1	22.4 ± 5.4	n.d.
2	22.6 ± 2.0	n.d.
3	36.8 ± 2.4	n.d.
4	31.2 ± 1.5	n.d.
5	20.5 ± 1.1	n.d.
6	36.9 ± 2.5	n.d.
7	43.5 ± 0.8	n.d.
8	44.3 ± 3.0	n.d.
9	60.0 ± 3.4	39.7 ± 0.9
10	17.2 ± 2.9	n.d.
11	19.1 ± 1.7	n.d.
12	22.5 ± 2.2	n.d.
13	34.0 ± 1.1	n.d.
14	33.1 ± 0.7	n.d.
17a	31.7 ± 1.8	n.d.
17b	28.7 ± 2.1	n.d.
17c	27.4 ± 4.2	n.d.
17d	24.0 ± 4.5	n.d.
17e	36.7 ± 2.1	n.d.
17f	36.0 ± 1.0	n.d.
17g	33.3 ± 2.3	n.d.
17h	28.3 ± 5.9	n.d.
17i	16.1 ± 3.0	n.d.
17j	14.0 ± 3.3	n.d.
17k	22.0 ± 1.4	n.d.
17l	n.i.	n.d.
F-3070	82.8 ± 1.3	22.3 ± 5.9
E-3205	40.2 ± 0.7	n.d.
F-3065	76.7 ± 2.4	24.6 ± 6.0

n.d., not determined.

n.i., no inhibition.

^a Percent inhibition was determined at 100 μM concentration of the indicated compound and represents an average of at least two independent measurements in duplicate.

^b The IC₅₀ values of the compounds were determined from dose-response curves employing 8–12 concentrations of each compound in duplicate in two independent experiments. Curves were fitted to data points using nonlinear regression analysis and IC₅₀ values were interpolated from the resulting curves using GraphPad Prism 3.03 software.

3070, and F-3065 having ≥60% anti-NS5B activity at 100 μM were further pursued for their IC₅₀ value determination. This analysis resulted in the identification of F-3070 and F-3065 with near similar IC₅₀ values, as the two most potent of the 36 STLC derivatives examined in this investigation, while **9** exhibited ~1.6–1.8-fold higher IC₅₀ value compared to the two afore-mentioned compounds. Together, these data suggest that STLC scaffold may offer further scope for improvement of its anti-NS5B activity.

To evaluate the anti-HCV activity of STLC compounds in a more biologically relevant setting, we employed the BHK-NS5B-FRLuc reporter and the Huh7/Rep-Feo1b reporter systems [36,37]. The former reporter system carries stably transfected NS5B and a bicistronic reporter gene, (+)FLuc-(−)UTR-RLuc for cell based investigations of HCV NS5B RdRp inhibitors [36]. The advantage of this system is that it can simultaneously measure intracellular HCV NS5B RdRp activity as reflected by the ratio of *Renilla* to firefly luciferase luminescence and cellular viability which is reflected by the firefly luciferase luminescence, thus enabling the identification of potent non-toxic inhibitors. The Huh7/Rep-Feo1b reporter system, on the other hand, autonomously replicates the subgenomic HCV genotype 1b replicon RNA carrying the firefly luciferase

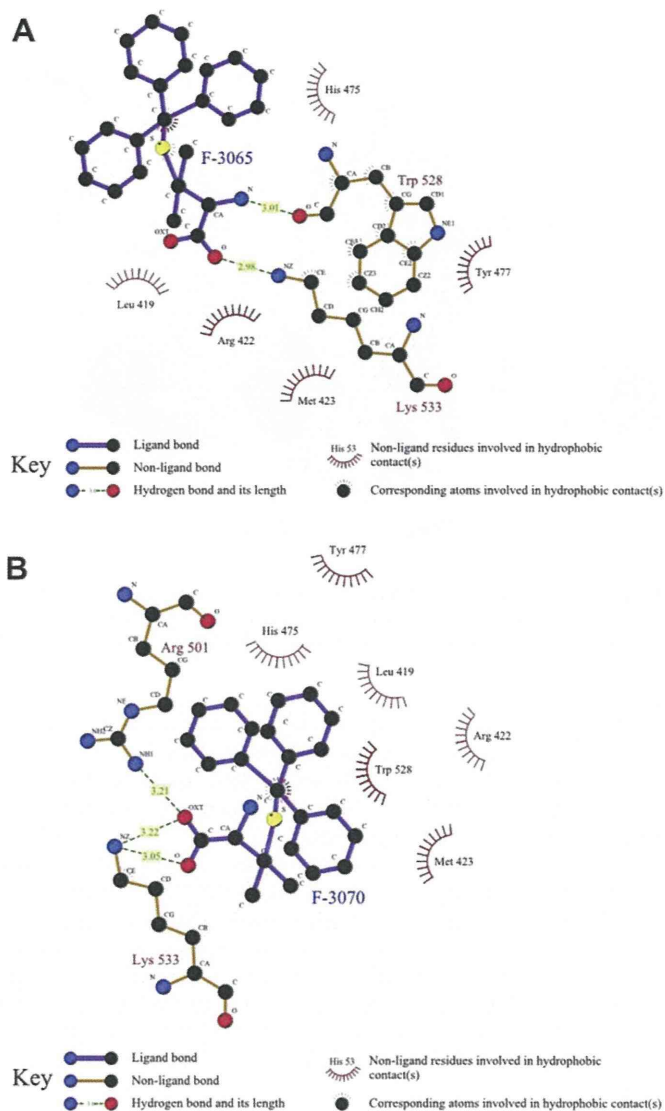


Fig. 3. Panel A: Ligplot diagram for F-3065 docked in NS5B (PDB ID 2d3u). Panel B: Ligplot diagram for F-3070 docked in NS5B (PDB ID 2d3u).

reporter as an indicator of HCV RNA replication, and has been widely employed to identify inhibitors of HCV RNA replication [37].

Only three STLC derivatives F-3070, F-3065, and E-3205 inhibited intracellular NS5B RdRp activity in the BHK-NS5B-FRLuc reporter at 100 μM concentration (Table 2). The two more potent of these, F-3070 and F-3065 exhibited ≥84% inhibition while E-3205 displayed only ~44% inhibition of NS5B RdRp activity, consistent with the in vitro data. In terms of their cytotoxicity parameters, F-3070 and F-3065 did not affect cell viability at 100 μM, as was evident from equivalent levels of firefly luciferase luminescence in compound treated cells versus DMSO controls. Treatment with E-3205 however, decreased cell viability by ~70% at 100 μM concentration. The remaining thirty-three STLC derivatives as well as the parent molecule, exhibited ≥50% reduction in cell viability at 100 μM, with only a marginal 15–30% decrease in intracellular NS5B activity (data not shown), consistent with the in vitro RdRp data.

In the Huh7/Rep-Feo1b reporter system, compounds F-3070 and F-3065 exhibited an overall similar pattern of cell viability and HCV RNA replication inhibition, corresponding to ~73–74% and ~89–91%, respectively at 100 μM concentration (Table 2). E-3205,

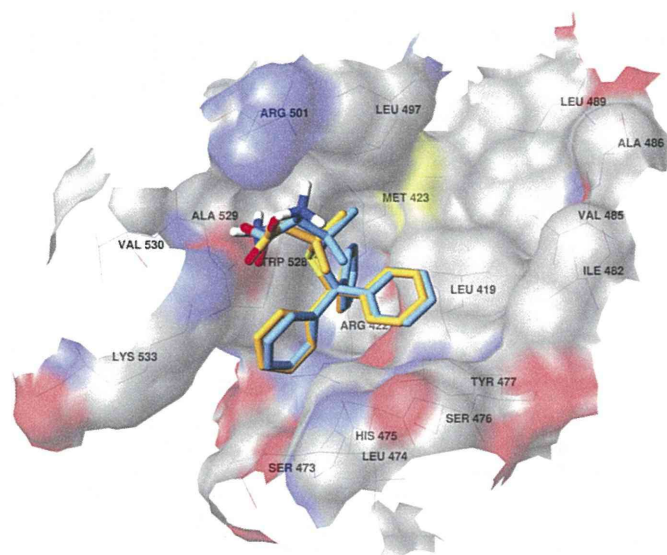


Fig. 4. Docked conformation of F-3065 (orange) and F-3070 (cyan) in NS5B (PDB ID 2d3u). The enzyme surface is shown in atom type color. (For interpretation of the references to colour in this figure legend, the reader is referred to the web version of this article.)

however, exhibited decreased cell viability (44%) compared to the other two compounds, though its inhibition of HCV RNA replication (~89%) was similar. It is worth noting here that the inhibition observed in this system may be partly attributed to the cellular toxicity effects of these compounds.

The results in this present study suggest that STLC derivatives inhibit HCV RNA replication by targeting the NS5B polymerase. It is possible that other host factors such as HMKEg are also targeted by STLCs in the HCV replicase complex and needs to be elucidated. These studies provide a platform to optimize the STLC scaffold as a potent anti-NS5B inhibitor. An extensive focused virtual screening approach is ongoing on a database constituted of more than 500 K trityl cysteine analogs to optimize the newly reported lead compounds.

3. Conclusion

In summary, STLC derivatives were identified as novel inhibitors of HCV NS5B polymerase activity in vitro and in cell based assays.

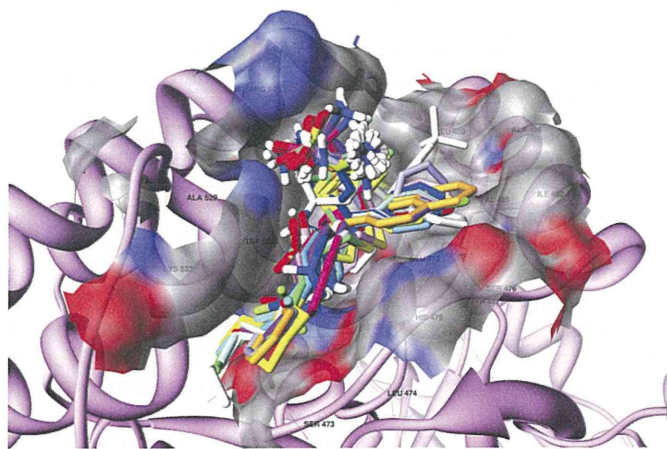


Fig. 5. STLC analogues docked within the HCV NS5B (in pink ribbon) thumb allosteric surface. The compounds overlap in this pocket. (For interpretation of the references to colour in this figure legend, the reader is referred to the web version of this article.)

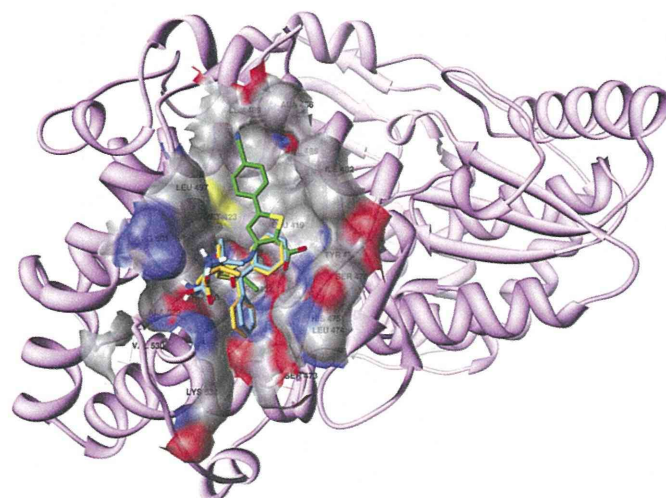


Fig. 6. F-3065 (orange) and F-3070 (cyan) overlapped on the 2d3u co-crystallized ligand (green). HCV NS5B (PDB ID 2d3u, in pink ribbon) and the thumb allosteric surface (in atom type color) are also shown. (For interpretation of the references to colour in this figure legend, the reader is referred to the web version of this article.)

This study validates structure-based molecular modeling coupled with 3-D QSAR prediction, as a viable strategy for identification of new structural scaffolds targeting NS5B. STLC binding mode analysis revealed a common way by which STLCs bind to the HCV NS5B thumb allosteric site and further suggested that improved STLC derivatives may be achieved by chemical modification at one of the trityl phenyl ring.

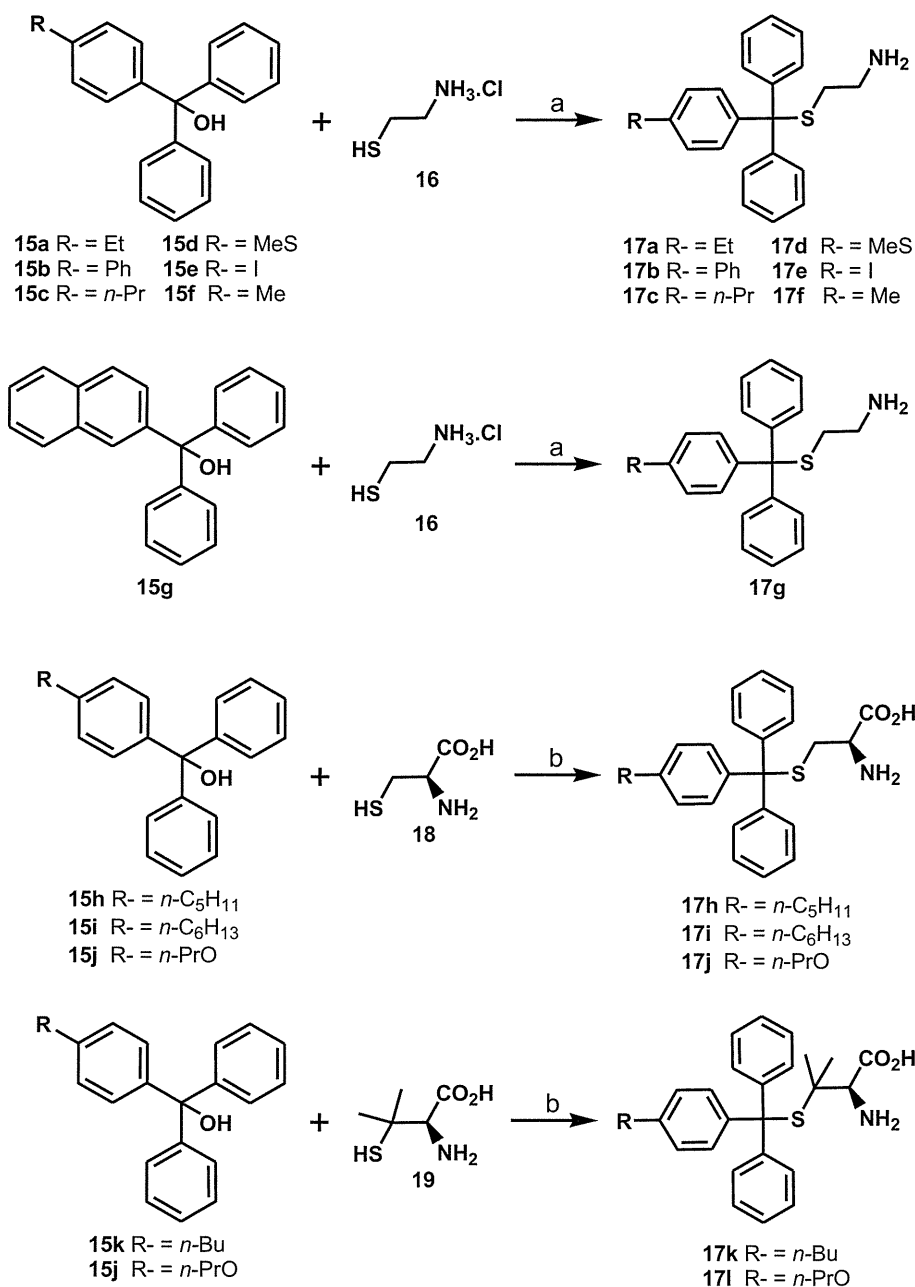
4. Experimental section

4.1. Molecular modeling

All molecules were generated by means of molecular mechanics of Chemaxon Marvin software (<http://www.chemaxon.com/>). Molecular graphics images were produced using UCSF Chimera package from the Resource for Biocomputing, Visualization, and Informatics at the University of California, San Francisco on a 3 GHz AMD CPU equipped IBM-compatible workstation with the Debian 5.0 version of the Linux operating system. Different from the previous protocol, the faster Autodock Vina [38] docking program was used in place of Autodock for all docking studies. Docking assessment was conducted via re-docking, re-docking modeled, cross-docking and cross-docking modeled as previously reported [26]. Autodock Vina proved to be as good as Autodock (data not shown), but much faster in calculations. The compounds were then submitted for structure-based molecular alignment through cross-docking protocols as previously reported [26]. For activity predictions, the previously developed SB 3-D QSAR model was applied without any modification [26]. The program ligplot v. 4.0 was used [39] to generate the ligand/NS5B interaction maps.

4.2. Chemistry

General methods: Melting points were determined using a Büchi capillary instrument and are uncorrected. Optical rotations were measured at the sodium D line (589 nm) at 25 °C with a Perkin–Elmer 241 polarimeter using a 1 dm path length cell. ^1H and ^{13}C NMR spectra were recorded on a Bruker 300, 400 or 500 MHz spectrometers. Chemical shifts (δ) are in parts per million. The following abbreviations were used to designate the multiplicities: s = singlet, d = doublet, t = triplet, q = quartet, m = multiplet, br = broad. Mass spectra were recorded with a Perkin–Elmer SCIEX



Scheme 1. Synthesis of STLC derivatives **17a–l**. Reagents and conditions: (a) TFA, rt, 3 h; (b) BF₃·Et₂O, AcOH, rt, 2 h.

API spectrometer. Elemental analyses were performed on a Thermoquest Flash 1112 series EA analyzer. Elemental analyses were found to be within ± 0.4 of the theoretical values. Purity of tested compounds was $>95\%$. All commercially available reagents and solvents were used without further purification. STLC and derivatives **1–14** have been previously described [29]. E-3205, F-3070 and F-3065 were purchased from Bachem. STDC (NSC124676), NSC123139, NSC136870, NSC140909, NSC123529, NSC123138, and NSC126217 were procured from NCI/NIH.

4.2.1. General procedure for preparation of compounds **17a–g**

At 0 °C and under argon atmosphere, a solution of cysteamine HCl (**16**) (1.33 mmol) was added dropwise to a solution of appropriate alcohol **15** (1.33 mmol) in TFA (5 mL). The reaction mixture was stirred at room temperature for 1 h, evaporated and extracted with a saturated solution of NaHCO₃(aq) and EtOAc. The organic

Table 2
Anti-HCV effects of STLC derivatives in cell based reporter assay.

Compound	BHK-NS5B-FR Luc ^a		Huh7/Rep-Feo1b ^b	
	Viability (%)	Inhibition (%)	Viability (%)	Inhibition (%)
F-3070	100.0	85.4	72.6	89.5
E-3205	30.2	44.4	44.2	88.6
F-3065	100.0	84.3	74.1	91.2

^aBHK-NS5B-FRLuc and ^bHuh7/Rep-Feo1b reporter cells were treated with the indicated compounds at 100 μ M concentration for 42 h. Cell viability in the BHK-NS5B-FRLuc reporter^a was estimated as the relative levels of Firefly luciferase in compound treated cells versus DMSO controls, while that in the Huh7/Rep-Feo1b cells^b was evaluated by the MTS assay. The inhibitory effect of the compounds on NS5B RdRp activity^a and HCV RNA replication^b is presented as percent of DMSO treated controls. Data represents an average of three independent experiments in duplicate.

phase was dried over MgSO₄, filtered, and evaporated under vacuum. The oil was crystallized from Et₂O or Et₂O/pentane 1:1. The desired compounds **17a–g** were obtained by filtration in the range of 29–47% yield.

4.2.1.1. 2-[1-(4-Ethylphenyl)-1,1-diphenylmethylthio]ethanamine (17a). Starting alcohol = 1-(4-ethylphenyl)-1,1-diphenylmethanol (**15a**). Yield: 31%; mp 138–140 °C; ¹H NMR (300 MHz, CD₃OD + D₂O): δ 1.23 (t, 3H, *J* = 7.5 Hz, CH₃), 2.45–2.59 (m, 4H, 2 CH₂), 2.58 (q, 2H, *J* = 7.5 Hz, CH₂), 7.17 (d, 2H, *J* = 8.5 Hz, H_{Ar}), 7.22–7.35 (m, 8H, H_{Ar}), 7.43–7.46 (m, 4H, H_{Ar}); ¹³C NMR (100 MHz, DMSO-*d*₆): δ 15.3 (CH₃), 27.6 (CH₂), 28.6 (CH₂), 37.7 (CH₂), 66.2 (Cq), 126.9 (2× CH), 127.5 (2× CH), 128.2 (4× CH), 129.0 (6× CH), 141.3 (Cq), 142.3 (Cq), 144.2 (2× Cq); MS (ESI): *m/z* 370 [M + Na]⁺; Anal. Calcd for C₂₃H₂₅NS: C 79.49, H 7.25, N 4.03, found: C 79.47, H 7.20, N 3.97.

4.2.1.2. 2-[1,1-Diphenyl-4-(phenyl)phenylmethylthio]ethanamine (17b). Starting alcohol = 1-(4-phenylphenyl)-1,1-diphenylmethanol (**15b**). Yield: 30%; mp 160–162 °C; ¹H NMR (300 MHz, CD₃OD + D₂O): δ 2.50–2.62 (s, 4H, 2 CH₂), 7.27–7.63 (m, 19H, H_{Ar}); ¹³C NMR (125 MHz, DMSO-*d*₆): δ 28.7 (CH₂), 37.8 (CH₂), 66.2 (Cq), 126.4 (2× CH), 126.6 (2× CH), 127.0 (2× CH), 127.6 (CH), 128.3 (4× CH), 128.9 (2× CH), 129.0 (4× CH), 129.6 (2× CH), 138.6 (Cq), 139.2 (Cq), 143.2 (Cq), 143.9 (2× Cq); MS (ESI): *m/z* 418 [M + Na]⁺; Anal. Calcd for C₂₇H₂₅NS: C 81.98, H 6.37; N 3.54, found: C 82.26, H 6.44, N 3.73.

4.2.1.3. 2-[1,1-Diphenyl-4-(propyl)phenylmethylthio]ethanamine (17c). Starting alcohol = 1,1-diphenyl-1-(4-propylphenyl) methanol (**15c**). Yield: 45%; mp 133–135 °C; ¹H NMR (300 MHz, CD₃OD + D₂O): δ 0.94 (t, 3H, *J* = 7.3 Hz, CH₃), 1.58–1.70 (m, 2H, CH₂), 2.45–2.49 (m, 2H, CH₂), 2.50–2.60 (m, 4H, CH₂), 7.14 (d, 2H, *J* = 8.3 Hz, H_{Ar}), 7.22–7.34 (m, 8H, H_{Ar}), 7.42–7.45 (m, 4H, H_{Ar}); ¹³C NMR (100 MHz, DMSO-*d*₆): δ 13.8 (CH₃), 23.9 (CH₂), 28.6 (CH₂), 36.7 (CH₂), 37.7 (CH₂), 66.2 (Cq), 126.9 (2× CH), 128.1 (2× CH), 128.2 (4× CH), 128.9 (2× CH), 129.0 (4× CH), 140.8 (Cq), 141.3 (Cq), 144.2 (2× Cq); MS (ESI): *m/z* 384 [M + Na]⁺; Anal. Calcd for C₂₄H₂₇NS: C 79.73, H 7.53, N 3.87, found: C 79.55, H 7.40, N 3.82.

4.2.1.4. 2-[1,1-Diphenyl-4-(methylthio)phenylmethylthio]ethanamine (17d). Starting alcohol = 1,1-diphenyl-1-(4-methylthiophenyl)methanol (**15d**). Yield: 40%; mp 142–144 °C; ¹H NMR (300 MHz, CD₃OD + D₂O): δ 2.47 (s, 3H, CH₃), 2.50–2.59 (m, 4H, CH₂), 7.20–7.37 (m, 10H, H_{Ar}), 7.43–7.46 (m, 4H, H_{Ar}); ¹³C NMR (125 MHz, DMSO-*d*₆): δ 14.3 (CH₃), 28.6 (CH₂), 37.7 (CH₂), 66.0 (Cq), 125.3 (2× CH), 127.0 (2× CH), 128.2 (4× CH), 128.9 (4× CH), 129.6 (2× CH), 137.0 (Cq), 140.3 (Cq), 143.9 (2× Cq); MS (ESI): *m/z* 388 [M + Na]⁺; Anal. Calcd for C₂₂H₂₃NS₂: C 72.28, H 6.34, N 3.83, found: C 72.00, H 6.35, N 3.77.

4.2.1.5. 2-[1-(4-Iodophenyl)-1,1-diphenylmethylthio]ethanamine (17e). Starting alcohol = 1-(4-iodophenyl)-1,1-diphenylmethanol (**15e**). Yield: 47%; mp 150–152 °C; ¹H NMR (300 MHz, CD₃OD + D₂O): δ 2.54 (s, 4H, 2 CH₂), 7.21–7.36 (m, 8H, H_{Ar}), 7.41–7.44 (m, 4H, H_{Ar}), 7.68 (d, 2H, *J* = 10.8 Hz, H_{Ar}); ¹³C NMR (125 MHz, DMSO-*d*₆): δ 28.8 (CH₂), 37.7 (CH₂), 66.0 (Cq), 93.4 (Cq), 127.1 (2× CH), 128.3 (4× CH), 128.9 (4× CH), 131.4 (2× CH), 137.0 (2× CH), 143.5 (2× Cq), 143.8 (Cq); MS (ESI): *m/z* 468 [M + Na]⁺; Anal. Calcd for C₂₁H₂₀I NS: C 56.63, H 4.53, N 3.15, found: C 56.60, H 4.61, N 3.22.

4.2.1.6. 2-[1-(4-Methylphenyl)-1,1-diphenylmethylthio]ethanamine (17f). Starting alcohol = 1-(4-methylphenyl)-1,1-diphenylmethanol (**15f**). Yield: 29%; mp 138–140 °C; ¹H NMR (300 MHz, CD₃OD + D₂O): δ 2.32 (s, 3H, CH₃), 2.48–2.55 (m, 4H, 2 CH₂), 7.13 (d, 2H, *J* = 8.1 Hz,

H_{Ar}), 7.24–7.34 (m, 8H, H_{Ar}), 7.41–7.45 (m, 4H, H_{Ar}); ¹³C NMR (100 MHz, DMSO-*d*₆): δ 20.5 (CH₃), 29.0 (CH₂), 37.9 (CH₂), 66.2 (Cq), 126.9 (2× CH), 128.2 (4× CH), 128.7 (2× CH), 129.0 (6× CH), 136.1 (Cq), 141.1 (Cq), 144.2 (2× Cq); MS (ESI): *m/z* 356 [M + Na]⁺; Anal. Calcd for C₂₂H₂₃NS: C 79.23, H 6.95, N 4.20, found: C 78.88, H 7.03, N 4.19.

4.2.1.7. 2-[1-(2-Naphthyl)-1,1-(diphenyl)methylthio]ethanamine (17g). Starting alcohol = 1-(2-naphthyl)-1,1-diphenylmethanol (**15g**) [32,40]. Yield: 32%; mp 126–128 °C; ¹H NMR (300 MHz, CD₃OD + D₂O): δ 2.34–2.47 (s, 4H, 2 CH₂), 7.21–7.34 (m, 6H, H_{Ar}), 7.43–7.49 (m, 6H, H_{Ar}), 7.55 (dd, 1H, *J* = 1.9, 8.9 Hz, H_{Ar}), 7.70–7.83 (m, 4H, H_{Ar}); ¹³C NMR (100 MHz, DMSO-*d*₆): δ 35.6 (CH₂), 40.8 (CH₂), 66.0 (Cq), 126.4 (CH), 126.5 (CH), 126.8 (2× CH), 127.2 (CH), 127.3 (CH), 127.5 (CH), 128.1 (5× CH), 128.2 (CH), 129.1 (4× CH), 131.6 (Cq), 132.3 (Cq), 141.9 (Cq), 144.5 (2× Cq); MS (ESI): *m/z* 392 [M + Na]⁺; Anal. Calcd for C₂₅H₂₃NS: C 81.26, H 6.27, N 3.79, found: C 81.38, H 6.31, N 3.89.

4.2.2. General procedure for preparation of compounds **17h–I**

At 0 °C and under argon atmosphere, a solution of BF₃·Et₂O (1.33 mmol) was added dropwise to a solution of appropriate alcohol **15** (0.86 mmol), *L*-cysteine (**18**) or *L*-penicillamine (**19**) (0.77 mmol) in AcOH (1 mL). The reaction mixture was stirred at room temperature for 3 h. Addition of 10% solution of NaOAc (2 mL), then H₂O (2 mL) led to the formation of a gum. After elimination of the supernatant, the final compound was precipitated by addition of pentane or Et₂O. The desired compounds **17h–I** were obtained by filtration in the range of 30–55% yield.

4.2.2.1. S-[1-(4-Pentylphenyl)-1,1-diphenylmethyl]-L-cysteine (17h). Starting alcohol = 1-(4-pentylphenyl)-1,1-diphenylmethanol (**15h**). Yield: 55%; mp 127–129 °C; [α]_D²⁵ = +61 (*c* = 0.52 in MeOH); ¹H NMR (300 MHz, CD₃OD + D₂O): δ 0.91 (t, 3H, *J* = 6.7 Hz, CH₃), 1.32–1.39 (m, 4H, 2 CH₂), 1.56–1.66 (m, 2H, CH₂), 2.59 (broad t, 2H, *J* = 7.9 Hz, CH₂), 2.70 (dd, 1H, *J* = 9.2, 13.5 Hz, CH₂), 2.82 (dd, 1H, *J* = 4.2, 13.5 Hz, CH₂), 3.04 (dd, 1H, *J* = 4.2, 9.2 Hz, CH), 7.13 (d, 2H, *J* = 8.5 Hz, H_{Ar}), 7.20–7.35 (m, 8H, H_{Ar}), 7.43–7.46 (m, 4H, H_{Ar}); ¹³C NMR (100 MHz, CD₃OD): δ 14.4 (CH₃), 23.6 (CH₂), 32.3 (CH₂), 32.7 (CH₂), 34.0 (CH₂), 36.4 (CH₂), 54.6 (CH), 68.0 (Cq), 128.0 (2× CH), 129.1 (6× CH), 130.6 (2× CH), 130.7 (4× CH), 142.8 (Cq), 143.0 (Cq), 145.8 (2× Cq), 172.0 (CO); MS (ESI): *m/z* 456 [M + Na]⁺; Anal. Calcd for C₂₇H₃₁NO₂S: C 74.79, H 7.21, N 3.23, found: C 74.79, H 7.17, N 3.25.

4.2.2.2. S-[1-(4-Hexylphenyl)-1,1-diphenylmethyl]-L-cysteine (17i). Starting alcohol = 1-(4-hexylphenyl)-1,1-diphenylmethanol (**15i**). Yield: 40%; mp 129–131 °C; [α]_D²⁵ = +53 (*c* = 0.54 in MeOH). ¹H NMR (300 MHz, CD₃OD + D₂O): δ 0.90 (t, 3H, *J* = 6.7 Hz, CH₃), 1.30–1.42 (m, 6H, 3 CH₂), 1.54–1.66 (m, 2H, CH₂), 2.59 (broad t, 2H, *J* = 7.9 Hz, CH₂), 2.70 (dd, 1H, *J* = 9.2, 13.5 Hz, CH₂), 2.82 (dd, 1H, *J* = 4.2, 13.5 Hz, CH₂), 3.03 (dd, 1H, *J* = 4.2, 9.2 Hz, CH), 7.12 (d, 2H, *J* = 8.3 Hz, H_{Ar}), 7.21–7.35 (m, 8H, H_{Ar}), 7.43–7.46 (m, 4H, H_{Ar}); ¹³C NMR (100 MHz, CD₃OD): δ 14.4 (CH₃), 23.7 (CH₂), 30.1 (CH₂), 32.5 (CH₂), 32.8 (CH₂), 34.0 (CH₂), 36.4 (CH₂), 54.7 (CH), 68.0 (Cq), 128.0 (2× CH), 129.1 (6× CH), 130.6 (2× CH), 130.7 (4× CH), 142.8 (Cq), 143.0 (Cq), 145.8 (2× Cq), 172.0 (CO); MS (ESI): *m/z* 470 [M + Na]⁺; Anal. Calcd for C₂₈H₃₃NO₂S: C 75.13, H 7.43, N 3.13, found: C 74.87, H 7.30, N 3.02.

4.2.2.3. S-[1,1-Diphenyl-1-(4-propoxyphenyl)methyl]-L-cysteine (17j). Starting alcohol = 1,1-diphenyl-1-(4-propoxyphenyl)methanol (**15j**) [41]. Yield: 43%; mp 144–146 °C; [α]_D²⁵ = +60 (*c* = 0.51 in MeOH); ¹H NMR (300 MHz, CD₃OD + D₂O): δ 1.03 (t, 3H, *J* = 7.3 Hz, CH₃), 1.72–1.84 (m, 2H, CH₂), 2.68 (dd, 1H, *J* = 9.2, 13.4 Hz, CH₂), 2.83 (dd,

1H, $J = 4.0, 13.4$ Hz, CH₂), 3.04 (dd, 1H, $J = 4.0, 9.2$ Hz, CH), 3.92 (t, 2H, $J = 6.4$ Hz, CH₂), 6.92 (d, 2H, $J = 8.8$ Hz, H_{Ar}), 7.22–7.33 (m, 8H, H_{Ar}), 7.43–7.45 (m, 4H, H_{Ar}); ¹³C NMR (100 MHz, CD₃OD): δ 10.8 (CH₃), 23.6 (CH₂), 34.2 (CH₂), 55.0 (CH), 67.7 (Cq), 70.5 (CH₂), 114.9 (2 \times CH), 127.9 (2 \times CH), 129.1 (4 \times CH), 130.5 (4 \times CH), 132.0 (2 \times CH), 137.2 (Cq), 146.0 (Cq), 146.1 (Cq), 159.3 (Cq), 172.3 (CO); MS (ESI): m/z 444 [M + Na]⁺; Anal. Calcd for C₂₅H₂₇NO₃S: C 71.23, H 6.46, N 3.32, found: C 71.44, H 6.54, N 3.30.

4.2.2.4. *S*-[1-(4-Butylphenyl)-1,1-diphenylmethyl]-L-penicillamine (**17k**). Starting alcohol = 1-(4-butylphenyl)-1,1-diphenylmethanol (**15k**). Yield: 30%; mp 123–125 °C; $[\alpha]_{589}^{25} = +171$ ($c = 0.54$ in MeOH); ¹H NMR (300 MHz, CD₃OD + D₂O): δ 0.93 (t, 3H, $J = 7.3$ Hz, CH₃), 1.30 (s, 3H, CH₃), 1.32–1.40 (m, 2H, CH₂), 1.42 (s, 3H, CH₃), 1.54–1.64 (m, 2H, CH₂), 1.85 (s, 1H, CH), 2.59 (t, 2H, $J = 7.5$ Hz, CH₂), 7.14 (d, 2H, $J = 8.3$ Hz, H_{Ar}), 7.19–7.34 (m, 6H, H_{Ar}), 7.56 (d, 2H, $J = 8.5$ Hz, H_{Ar}), 7.67–7.70 (m, 4H, H_{Ar}); ¹³C NMR (100 MHz, CD₃OD): δ 14.3 (CH₃), 23.4 (CH₂), 25.9 (CH₃), 27.9 (CH₃), 34.7 (CH₂), 36.1 (CH₂), 53.5 (Cq), 61.9 (CH), 69.2 (Cq), 127.9 (2 \times CH), 129.0 (6 \times CH), 130.7 (2 \times CH), 130.8 (2 \times CH), 130.9 (2 \times CH), 142.9 (Cq), 143.2 (Cq), 146.0 (Cq), 146.1 (Cq), 170.6 (CO); MS (ESI): m/z 470 [M + Na]⁺; Anal. Calcd for C₂₈H₃₃NO₂S: C 75.13, H 7.43, N 3.13, found: C 75.45, H 7.53, N 3.32.

4.2.2.5. *S*-[1,1-Diphenyl-1-(4-propoxyphenyl)methyl]-L-penicillamine (**17l**). Starting alcohol = 1,1-diphenyl-1-(4-propoxyphenyl)methanol (**15j**). Yield: 34%; mp 133–135 °C; $[\alpha]_{589}^{25} = +69$ ($c = 0.15$ in MeOH); ¹H NMR (300 MHz, CD₃OD + D₂O): δ 1.03 (t, 3H, $J = 7.1$ Hz, CH₃), 1.31 (s, 3H, CH₃), 1.43 (s, 3H, CH₃), 1.74–1.81 (m, 2H, CH₂), 1.92 (s, 1H, CH), 3.93 (t, 2H, $J = 6.0$ Hz, CH₂), 6.87 (d, 2H, $J = 8.4$ Hz, H_{Ar}), 7.20–7.30 (m, 6H, H_{Ar}), 7.56 (d, 2H, $J = 8.4$ Hz, H_{Ar}), 7.64–7.72 (m, 4H, H_{Ar}); ¹³C NMR (100 MHz, CD₃OD): δ 10.8 (CH₃), 23.7 (CH₂), 25.9 (CH₃), 28.4 (CH₃), 53.2 (Cq), 62.0 (CH), 69.2 (Cq), 70.5 (CH₂), 114.6 (2 \times CH), 127.8 (2 \times CH), 128.7 (4 \times CH), 129.5 (4 \times CH), 131.6 (2 \times CH), 137.3 (Cq), 146.0 (2 \times Cq), 159.6 (Cq), 172.6 (CO); MS (ESI): m/z 472 [M + Na]⁺; Anal. Calcd for C₂₇H₃₁NO₃S: C 72.13, H 6.95, N 3.12, found: C 71.99, H 7.00, N 3.11.

4.3. Biological studies

4.3.1. NS5B inhibition assay

Recombinant NS5B carrying the N-terminal histidine-tag was purified from the plasmid pThNS5BC Δ 21 expressed in *Escherichia coli* DH5 α by Ni-NTA chromatography [33,34]. The compounds were dissolved in dimethylsulfoxide (DMSO) as a 10 mM stock solution and stored at –20 °C. Serial dilutions were made in DMSO immediately prior to the assay. The activity of the compounds against HCV NS5B was evaluated by the standard primer dependent elongation assay as previously described [33,34]. Briefly, preliminary screening was performed in the presence or absence of 100 μ M STL or the indicated derivative in a reaction buffer containing 20 mM Tris–HCl (pH 7.0), 100 mM NaCl, 100 mM Na-glutamate, 0.1 mM DTT, 0.01% BSA, 0.01% Tween-20, 5% glycerol, 20 U/mL of RNasin, 20 μ M UTP, 2 μ Ci [α -³²P]UTP, 0.25 μ M polyA/U₁₂, 100 ng NS5BC Δ 21 and 1 mM MnCl₂. Following 60 min incubation at 30 °C, reactions were terminated by the addition of chilled 5% trichloroacetic acid (TCA) containing 0.5 mM sodium pyrophosphate. Reaction products were precipitated on GF-B filters and quantified on a liquid scintillation counter. NS5B activity in the presence of DMSO control was set at 100% and that in the presence of the STL derivatives was determined relative to this control. Compounds exhibiting greater than 50% inhibition at 100 μ M were evaluated for their IC₅₀ values from dose-response curves employing 8–12 concentrations of the compounds in duplicate in two independent experiments. Curves were fitted to data points

using nonlinear regression analysis and IC₅₀ values were interpolated from the dose-response curves using GraphPad Prism 3.03 software.

4.3.2. Cell culture

BHK-NS5B-FRLuc reporter cells were grown in Dulbecco's modified Eagle's medium (DMEM) with 10% heat-inactivated fetal bovine serum, 5% antibiotic-antimycotic, 5% nonessential amino acid, 1 mg/mL G418 and 10 μ g/mL blasticidin. Huh7/Rep-Feo1b replicon reporter cells were cultivated in DMEM containing 10% fetal calf serum, 5% antibiotic and 0.5 mg/mL G418. All cell lines were incubated at 37 °C in the presence of 5% CO₂ supplement.

4.3.3. BHK-NS5B-FRLuc reporter assay

The effect of the compounds on intracellular NS5B RdRp activity was screened employing the BHK-NS5B-FRLuc reporter system as previously described [36]. Briefly, BHK-NS5B-FRLuc reporter cells were plated at a confluence of 1×10^4 cells/well in 96 well plates and incubated with DMSO (1%) or the indicated compound (100 μ M) for 42 h. Reporter gene expression was measured with a Dual-Glo Luciferase Assay Kit (Promega, USA) in accordance with the manufacturer's instructions. Effect of the compounds on cell viability was estimated as the relative levels of firefly luciferase in compound treated cells versus DMSO controls. The inhibitory effect of the compounds on the intracellular NS5B RdRp activity was evaluated from the percent reduction in RLuc to FLuc luminescence signal in compound treated cells versus DMSO controls.

4.3.4. Huh7/Rep-Feo1b reporter system

The effect of the compounds on HCV RNA replication was screened employing the Huh7/Rep-Feo1b replicon reporter cells as previously described [42]. Briefly, 1×10^4 Huh7/Rep-Feo1b cells were plated in 96 well plates and treated with 100 μ M concentration of the indicated compound or DMSO for 42 h. The concentration of DMSO in cell culture was kept constant at 1.0%. Cell viability was measured by the colorimetric MTS assay employing the Cell-Titer 96AQ_{ueous} one solution assay reagent (Promega, USA). Inhibitory effect of the compounds on HCV RNA replication was measured as the relative levels of firefly luciferase signals in compound treated cells versus DMSO controls.

Acknowledgments

This work was supported by the National Institute of Health Research Grants DK066837 and CA153147 to N.K.-B. We would like to thank Prof. Garland R. Marshall (Washington University of St. Louis - MO) for critical reading of the manuscript.

References

- [1] A. Wasley, M.J. Alter, Epidemiology of hepatitis C: geographic differences and temporal trends, *Semin. Liver Dis.* 20 (2000) 1–16.
- [2] A. Grakoui, H.L. Hanson, C.M. Rice, Bad time for Bonzo? Experimental models of hepatitis C virus infection, replication, and pathogenesis, *Hepatology* 33 (2001) 489–495.
- [3] G.M. Lauer, B.D. Walker, Hepatitis C virus infection, *N. Engl. J. Med.* 345 (2001) 41–52.
- [4] I. Saito, T. Miyamura, A. Ohbayashi, H. Harada, T. Katayama, S. Kikuchi, Y. Watanabe, S. Koi, M. Onji, Y. Ohta, et al., Hepatitis C virus infection is associated with the development of hepatocellular carcinoma, *Proc. Natl. Acad. Sci. USA* 87 (1990) 6547–6549.
- [5] J. Ruiz, B. Sangro, J.I. Cuende, O. Beloqui, J.I. Riezu-Boj, J.I. Herrero, J. Prieto, Hepatitis B and C viral infections in patients with hepatocellular carcinoma, *Hepatology* 16 (1992) 637–641.
- [6] J.H. Hoofnagle, A.M. di Bisceglie, The treatment of chronic viral hepatitis, *N. Engl. J. Med.* 336 (1997) 347–356.
- [7] J.M. Pawlotsky, Pathophysiology of hepatitis C virus infection and related liver disease, *Trends Microbiol.* 12 (2004) 96–102.

- [8] J.J. Feld, T.J. Liang, HCV persistence: cure is still a four letter word, *Hepatology* 41 (2005) 23–25.
- [9] P. Ferenci, Pegylated interferon plus ribavirin for chronic hepatitis C: the role of combination therapy today, tomorrow and in the future, *Minerva Gastroenterol. Dietol.* 52 (2006) 157–174.
- [10] J.M. Pawlotsky, Virology of hepatitis B and C viruses and antiviral targets, *J. Hepatol.* 44 (2006) S10–S13.
- [11] C. Sheridan, New Merck and Vertex drugs raise standard of care in hepatitis C, *Nat. Biotechnol.* 29 (2011) 553–554.
- [12] C. Rice, Perspective: miles to go before we sleep, *Nature* 474 (2011) S8.
- [13] K. Garber, Hepatitis C: move over interferon, *Nat. Biotechnol.* 29 (2011) 963–966.
- [14] Q.L. Choo, G. Kuo, A.J. Weiner, L.R. Overby, D.W. Bradley, M. Houghton, Isolation of a cDNA clone derived from a blood-borne non-A, non-B viral hepatitis genome, *Science* 244 (1989) 359–362.
- [15] K. Tsukiyama-Kohara, N. Iizuka, M. Kohara, A. Nomoto, Internal ribosome entry site within hepatitis C virus RNA, *J. Virol.* 66 (1992) 1476–1483.
- [16] V. Brass, D. Moradpour, H.E. Blum, Molecular virology of hepatitis C virus (HCV): 2006 update, *Int. J. Med. Sci.* 3 (2006) 29–34.
- [17] S.E. Behrens, L. Tomei, R. De Francesco, Identification and properties of the RNA-dependent RNA polymerase of hepatitis C virus, *EMBO J.* 15 (1996) 12–22.
- [18] C.H. Hagedorn, E.H. van Beers, C. De Staercke, Hepatitis C virus RNA-dependent RNA polymerase (NS5B polymerase), *Curr. Top. Microbiol. Immunol.* 242 (2000) 225–260.
- [19] D. Moradpour, V. Brass, E. Bieck, P. Friebe, R. Gosert, H.E. Blum, R. Bartenschlager, F. Penin, V. Lohmann, Membrane association of the RNA-dependent RNA polymerase is essential for hepatitis C virus RNA replication, *J. Virol.* 78 (2004) 13278–13284.
- [20] R. De Francesco, C.M. Rice, New therapies on the horizon for hepatitis C: are we close? *Clin. Liver Dis.* 7 (2003) 211–242 (xi).
- [21] A.D. Kwong, L. McNair, I. Jacobson, S. George, Recent progress in the development of selected hepatitis C virus NS3.4A protease and NS5B polymerase inhibitors, *Curr. Opin. Pharmacol.* 8 (2008) 522–531.
- [22] S. Bressanelli, L. Tomei, A. Rousset, I. Incitti, R.L. Vitale, M. Mathieu, R. De Francesco, F.A. Rey, Crystal structure of the RNA-dependent RNA polymerase of hepatitis C virus, *Proc. Natl. Acad. Sci. USA* 96 (1999) 13034–13039.
- [23] C.A. Lesburg, M.B. Cable, E. Ferraris, Z. Hong, A.F. Mannarino, P.C. Weber, Crystal structure of the RNA-dependent RNA polymerase from hepatitis C virus reveals a fully encircled active site, *Nat. Struct. Biol.* 6 (1999) 937–943.
- [24] H. Ago, T. Adachi, A. Yoshida, M. Yamamoto, N. Habuka, K. Yatsunami, M. Miyano, Crystal structure of the RNA-dependent RNA polymerase of hepatitis C virus, *Structure* 7 (1999) 1417–1426.
- [25] S. Bressanelli, L. Tomei, F.A. Rey, R. De Francesco, Structural analysis of the hepatitis C virus RNA polymerase in complex with ribonucleotides, *J. Virol.* 76 (2002) 3482–3492.
- [26] I. Musmuca, A. Caroli, A. Mai, N. Kaushik-Basu, P. Arora, R. Ragno, Combining 3-D quantitative structure-activity relationship with ligand based and structure based alignment procedures for in silico screening of new hepatitis C virus NS5B polymerase inhibitors, *J. Chem. Inf. Model.* 50 (2010) 662–676.
- [27] J.E. Silverman, M. Ciustea, A.M. Shudofsky, F. Bender, R.H. Shoemaker, R.P. Ricciardi, Identification of polymerase and processivity inhibitors of vaccinia DNA synthesis using a stepwise screening approach, *Antivir. Res.* 80 (2008) 114–123.
- [28] K.Y. Zee-Cheng, C.C. Cheng, Experimental antileukemic agents. Preparation and structure-activity study of S-tritylcysteine and related compounds, *J. Med. Chem.* 13 (1970) 414–418.
- [29] S. Debonis, D.A. Skoufias, R.L. Indorato, F. Liger, B. Marquet, C. Laggner, B. Joseph, F. Kozielski, Structure-activity relationship of S-trityl-L-cysteine analogues as inhibitors of the human mitotic kinesin Eg5, *J. Med. Chem.* 51 (2008) 1115–1125.
- [30] H.Y. Kaan, D.D. Hackney, F. Kozielski, The structure of the kinesin-1 motor-tail complex reveals the mechanism of autoinhibition, *Science* 333 883–885, New York, N.Y.
- [31] H.Y. Kaan, J. Weiss, D. Menger, V. Ulaganathan, K. Tkocz, C. Laggner, F. Popowycz, B. Joseph, F. Kozielski, Structure-activity relationship and multidrug resistance study of new S-trityl-L-cysteine derivatives as inhibitors of Eg5, *J. Med. Chem.* 54 (2011) 1576–1586.
- [32] E. Weber, K. Skobridis, A. Wierig, I. Goldberg, Triarylmethanol host compounds. Synthesis, crystalline complex formation and X-ray crystal structures of three inclusions species, *J. Inclusion Phenom. Mol.* 28 (1997) 163–179.
- [33] N. Kaushik-Basu, A. Bopda-Waffo, T.T. Talele, A. Basu, Y. Chen, S.G. Kucukguzel, 4-Thiazolidinones: a novel class of hepatitis C virus NS5B polymerase inhibitors, *Front. Biosci.* 13 (2008) 3857–3868.
- [34] N. Kaushik-Basu, A. Bopda-Waffo, T.T. Talele, A. Basu, P.R. Costa, A.J. da Silva, S.G. Sarafianos, F. Noel, Identification and characterization of coumestans as novel HCV NS5B polymerase inhibitors, *Nucleic Acids Res.* 36 (2008) 1482–1496.
- [35] Y. Chen, A. Bopda-Waffo, A. Basu, R. Krishnan, E. Silberstein, D.R. Taylor, T.T. Talele, P. Arora, N. Kaushik-Basu, Characterization of aurintricarboxylic acid as a potent hepatitis C virus replicase inhibitor, *Antivir. Chem. Chemother.* 20 (2009) 19–36.
- [36] J.C. Lee, C.K. Tseng, K.J. Chen, K.J. Huang, C.K. Lin, Y.T. Lin, A cell-based reporter assay for inhibitor screening of hepatitis C virus RNA-dependent RNA polymerase, *Anal. Biochem.* 403 (2010) 52–62.
- [37] Y. Itsui, N. Sakamoto, S. Kakinuma, M. Nakagawa, Y. Sekine-Osajima, M. Tasaka-Fujita, Y. Nishimura-Sakurai, G. Suda, Y. Karakama, K. Mishima, M. Yamamoto, T. Watanabe, M. Ueyama, Y. Funaoka, S. Azuma, M. Watanabe, Antiviral effects of the interferon-induced protein guanylate binding protein 1 and its interaction with the hepatitis C virus NS5B protein, *Hepatol.* 50 (2009) 1727–1737 Baltimore, Md.
- [38] O. Trott, A.J. Olson, AutoDock Vina: improving the speed and accuracy of docking with a new scoring function, efficient optimization, and multithreading, *J. Comput. Chem.* 31 (2010) 455–461.
- [39] A.C. Wallace, R.A. Laskowski, J.M. Thornton, LIGPLOT: a program to generate schematic diagrams of protein-ligand interactions, *Protein Eng.* 8 (1995) 127–134.
- [40] J. Barluenga, F.J. Fananas, R. Sanz, C. Marcos, M. Trabada, On the reactivity of o-lithioaryl ethers: tandem anion translocation and Wittig rearrangement, *Org. Lett.* 4 (2002) 1587–1590.
- [41] Y. Kawakami, Y. Sakai, A. Okada, Synthesis and polymerization of mono-p-alkoxy-substituted triphenylmethyl acrylate, *Polym. J.* 22 (1990) 705–718.
- [42] K. Kim, K.H. Kim, H.Y. Kim, H.K. Cho, N. Sakamoto, J. Cheong, Curcumin inhibits hepatitis C virus replication via suppressing the Akt-SREBP-1 pathway, *FEBS Lett.* 584 (2010) 707–712.